Quasi-Optical Design of a Millimeter Wave Imaging System

Faeze Jadidi
Malek-Ashtar University of Technology https://orcid.org/0000-0002-7538-3160
Abdollah Eslamimajd (a_eslamimajd@mut-es.ac.ir)
Malek Ashtar University of Technology
Alireza Erfaniyan
Malek-Ashtar University of Technology
Seyed Hossein Mohseni Armaki
Malek-Ashtar University of Technology

Research

Keywords: Fresnel lens, millimeter wave imaging, aspheric lens, corrugated Gaussian horn antenna

Posted Date: November 5th, 2020

DOI: https://doi.org/10.21203/rs.3.rs-60526/v2

Quasi-Optical Design of a Millimeter Wave Imaging System

Faeze jadidi [1], Abdollah Eslamimajd[*2], Alireza Erfaniyan [3], Seyed Hossein Mohseni Armaki [3]

1: Malek Ashtar University of Technology, Faculty of Electrical & Computer, Department of Electrical Engineering, Lavizan, Tehran, Iran, 158751774, jadidi@mut.ac.ir

2: Malek Ashtar University of Technology, Faculty of Electrical & Computer, Department of Electrical Engineering, Lavizan, Tehran, Iran, 158751774, a_eslamimajd@mut-es.ac.ir

3: Malek Ashtar University of Technology, Faculty of Electrical & Computer, Department of Electrical Engineering, Lavizan, Tehran, Iran, 158751774

Abstract

In this paper, we report a complete design and simulation of a quasi-optical millimeter wave imaging system using ZEMAX and FEKO software, respectively. A Fresnel lens and a horn antenna are combined in this this design. Compared to spherical and aspherical lenses, a Fresnel lens can be fabricated much easier at millimeter wavelengths. For focusing millimeter wave radiation, a Fresnel lens can be used to reduce the thickness of the focusing element and to lighten its weight from 25 Kg to 4.5 Kg. A horn antenna with a Gaussian profile and corrugated walls is designed for feeding this system at a central frequency of 94 GHz. The symmetrical radiation pattern of the designed corrugated Gaussian horn in E and H orthogonal planes, its wide bandwidth and low side lobe levels make it a good candidate for feeding a W-band millimeter wave imaging system. The designed quasi-optical imaging system is light-weighted, has high resolution and can be used in detecting hidden objects within a distance of 5 meters with a 30 mm resolution in W-band at a central frequency of 94 GHz.

Keywords:

Fresnel lens, millimeter wave imaging, aspheric lens, corrugated Gaussian horn antenna

1- Introduction

Millimeter wave imaging systems have many applications from radio astronomy to defense and security [1]. This technology is capable of imaging under adverse climatic conditions and enables the detection of hidden objects [2]. New threats, including plastic/ceramic rifles and knives, are not detectable by metal detectors, as they can only detect metal targets. The effectiveness of metal detectors depends on the amount, direction, and the type of the metals. Additionally, metal detectors cannot distinguish between items such as glasses, belts, keys, and real threats, leading to false alarms [3].

Millimeter wave imaging technology is safe for living beings as compared to X-rays and has the potential to penetrate strongly into plastics, cardboard, textiles, and other materials used for packing. This feature is desired for security and detection of hidden weapons, as well as controlling passengers' luggage at airports and border points. Due to the unique features of millimeter waves in electromagnetic spectrum, including high penetration and low energy, millimeter wave technology is expanding rapidly [4,5]. The difference of millimeter wave and terahertz imaging is in their maturity of technology. Developing high-power sources and sensitive detectors in terahertz band is difficult. Moreover, the absorptions in solids can be attributed to vibrational modes. Lattice modes are the case in low frequencies; e.g., polythene has a lattice mode at 2.4 terahertz. Solids do not exhibit such absorptions in millimeter bands. Clothing is highly transparent in millimeter wave region, so hidden threats under clothing can be imaged. This can be achieved by imaging or sensing at 1 terahertz or above, where clothing is still relatively transparent. Indeed, the limitations imposed by atmospheric transmission severely affect the performance of terahertz systems at a fair stand-off range or in bad weather [6].

Millimeter waves cover a wavelength range of 1-10 mm, which corresponds to a frequency range of 30-300 GHz [7]. Regarding the atmospheric transmission, there are two optimal frequency bands (i.e., Q (35 GHz) and W (94 GHz) bands) for use in millimeter wave imaging. Frequency selection is based on a simple rule: selecting a lower frequency for greater penetration depth and optics with larger aperture, and/or selecting a higher frequency for better resolution. Compared to the Q-band, the W-band has better image quality and spatial resolution, which is controlled by the diffraction limit. The distance of the millimeter wave imaging system from the target is usually several meters [8].

The history of millimeter wave technology dates back to 1890, but the first important activity in this field was conducted in 1930 [9]. Ditchfield and England (1955) introduced the first millimeter wave imaging system in the UK [10]. Since then, technology has continued with rapid advances in recent years [11]. Dielectric lenses or reflectors can be used for imaging systems [6]. Of course, each of the two methods of refraction and reflection has advantages and disadvantages. Reflective systems are light in weight, but due to their smaller number of components and interconnection, they have narrower field of view than equivalent refractive systems, and the installation of mirrors in these systems is even more difficult [12]. At frequencies above 30 GHz, lens antennas can be considered as great alternative to reflectors since they are not affected by aperture blockage, exhibit great manufacturing tolerance and use inexpensive plastic materials. However, when a short focal length is accompanied by a large diameter, the thickness and weight of a lens are increased. These limitations can be avoided by using the diffractive equivalent of the lens, i.e., Fresnel zoned lens [13,14].

Fresnel zoned lenses are good options as focusing elements in the millimeter wave band. The lens material should have low values of loss, mass density and dielectric constant (ε_r=2-4) [15]. Millimeter wave band lenses are usually made of materials like high-density polyethylene (HDPE), silicon, polystyrene, Rexolite, and/or Teflon. HDPE is a cost-effective material and can be easily machined using computer-aided cutting [16,17]. A uniform dielectric lens with two surfaces is equivalent to two reflectors because each surface is equivalent to a degree of freedom. By forming both surfaces, the designers can design a lens that corrects aberrations [18].

The performance of highly accurate optical systems that use spherical optics is limited by aberrations. Using aspherical optics, geometric aberrations can be reduced or removed. New manufacturing methods allow producing high-precision aspherical surfaces [19]. Since quasi-optical imaging systems have to reduce the blurring effect for obtaining an acceptable sharpness, an aspherical lens can be used [8].

Zhou et al. (2015) developed a 43-cm diameter HDPE aspherical transition system at 89 GHz that was capable of imaging objects at a distance of 3.5 m with a resolution of 28 mm. Chen et al. reported a similar system with 35 mm resolution at a distance of 3.5 m [2,20]. In 2011, an HDPE transition system was developed with a diameter of 50 cm at 94 GHz using a one-dimensional array of receivers [21]. A focal array imaging system was also made in 2011 using an acrylic lens with a diameter of 20 cm and a resolution of 2 cm at a distance of 1 m in the frequency range 75-95 GHz [22].

In the millimeter wave band, where large lenses are required because of the diffraction limit, the system becomes very heavy [8]. When thinner, lighter, and easy-to-manufacture systems are required to focus the incoming radiation, Fresnel lenses are preferred over conventional refractive lenses. Fresnel lenses use diffraction as a method of collecting electromagnetic waves at the focal point. In this type of lens, the stepped discrete pattern, which first proposed by Rayleigh [23], can realize phase correction. According to this theory, different methods have been proposed and the desired phase correction has been achieved [23-25,17].

A 600 GHz Fresnel lens was designed for active and passive imaging by Chen et al. (2007) [1]. Design and manufacturing of Fresnel zone plate lenses with opaque and transparent zones at millimeter wavelengths was reported by Leon et al. (2014) [26]. Moreover, the use of dielectric Fresnel lenses for imaging was investigated in the frequency range 75-110 GHz in 2017 [27].

In passive systems, the target radiation is measured by the systems, while in active systems, a source is used to illuminate the target. An important application of passive imaging in millimeter wave region is the detection of weapons hidden under clothing [28]. In short-range stand-off passive millimeter wave imaging, the main purpose is to reduce the costs and complexity of the system [29]. Here, the optical configuration is arranged so that the optical aberration is reduced and the system can be employed in active or passive mode by proper setup.

Wide range applications of electromagnetic spectrum have made it necessary to use methods of designing and developing antennas for lowering the interference that may occur between the wanted signals and undesired ones. Many methods have been presented during recent years and a number of them have received attention and have been employed in real word applications. These methods can be divided into two broad categories: side lobe reduction and gain reduction in specific narrow directions, which is, in reality, null placement in the radiation patterns. Side lobes can cause noise in phase contrast image and some problems in hidden objects detection. The effect of this noise is considerable on the surface measurement and consequently on the uncertainty in measurement. This noise can be suppressed by a few enhancement techniques and many methods are available for side lobe reduction. Wavelet transform (WT) is an example of side lobe reduction methods that has been proposed for demodulation using the Fourier transform (FT) [30-32].

In quasi-optical systems, the free space energies are focused by the lens to a horn antenna, which transmits it to the detector as shown in fig. 1. There are different types of horn antennas with advantages and disadvantages that have to be taken into account when designing a quasi-optical system [33].

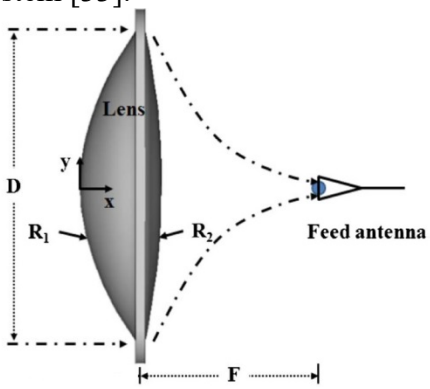

Fig. 1. Quasi-optics configuration consisting of a lens and feeding horn.

In millimeter wave region, high-performance applications, such as security imaging, radar, and radio astronomy, corrugated horn antennas are commonly used for feeding due to their high ray symmetry, relatively low side lobe levels, and low cross-polarization [34].

The process of designing a quasi-optical system involves the design of the primary optics (selection of focal element) and the secondary optics (selection of horn profile and wall surface features) according to the system requirements.

In this study, the primary optics is designed using an aspherical lens that has a better spot diagram and corrected aberrations as compared to spherical lenses. A grooved Fresnel lens is then simulated in the ZEMAX software to replace with the aspherical lens due to the heaviness of the aspherical lens. A corrugated Gaussian profile horn is also designed at a central frequency of 94 GHz as the secondary optics, and simulated using the electromagnetic software FEKO. This horn can be used with a lens (spherical, aspherical, or Fresnel lens) with an f-number of 1.2, to meet the requirements of the system. This system is capable of forming an image by mechanically scaning the object plane or using an array of detectors in the image plane with a spatial resolution of 30 mm at a distance of 5 m.

2- Result and Discussion

2-1 Aspherical lens

The spatial resolution in imaging applications is diffraction limited. The angle is limited by the diffraction corresponding to the central zone of the diffraction pattern, which comprises 84% of the irradiance distribution. According to Rayleigh's criterion, the optical system resolution is given in Equation (1).

$$s = R\frac{1.22\lambda}{D} \quad (1)$$

where λ is the central frequency, R is the imaging distance, D is the diameter of the input aperture and s is the resolution required at R [12]. According to Rayleigh's criterion, for

achieving a resolution of 30 mm at 94 GHz and a distance of 5 m, the aperture diameter should be about 65 cm.

The designed optical system is a transmission dielectric aspherical lens, which is simulated by the ZEMAX software (Fig. 2); this system consists of the object plane (left), lens and image plane (right). Moreover, the colored lines show different positions of the object in the field of view of the designed lens. HDPE lens dielectric material with a refractive index of 1.5147 is suitable for imaging (at 94 GHz, tanδ= 0.0003 and ε = 2.2). HDPE has not been listed in ZEMAX ™ Glass catalog, so it was entered in the frequency range 45-145 GHz using "appropriate coefficient data" and Conrady's formula according to Equation (2):

$$n(\lambda) = n_0 + \frac{A}{\lambda} + \frac{B}{\lambda^{3.5}} \quad (2)$$

Conrady's formula is a well-known equation for changing the refractive index of a material in the wavelength region, and uses three pairs of wavelength-refractive index data to create continuous capability [27].

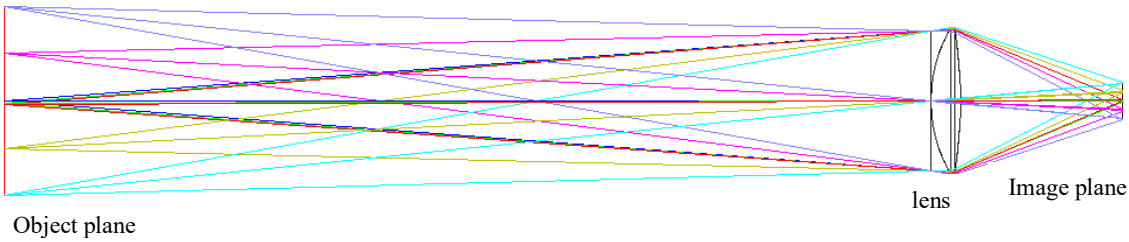

Fig. 2: Overview of the designed aspherical lens, consisting object plane (left), lens and image plane (right). The colors show different positions of object plane in field of view of the designed lens.

The formula of the aspherical lens surface is given as follows:

$$Z = \frac{c^{-1}r^2}{1+\sqrt{1-(1+k)c^{-2}r^2}} + \alpha_1 r^2 + \alpha_2 r^4 + \alpha_3 r^6 + \alpha_4 r^8 + \alpha_5 r^{10} \quad (3)$$

where c is the curvature, r is the radial coordinate, and k is the conic constant. Table 1 shows the optimized values of aspherical surface constants of the simulated lens according to ZEMAX. D and d, the diameter and thickness of the lens are 650 and 71 millimeters, respectively. Using these parameters and mass density, which were entered in ZEMAX, this lens weighs 25 kg.

Table 1: Aspherical lens design constants.

Parameter	Surface 1	Surface 2
C	921.542	-915.071
K	1.791	-71.404
α_1	2.38e-4	-1.343e-6
α_2	1.746e-9	-1.139e-10
α_3	-8.464e-15	-6.672e-16
α_4	-4.151e-21	-9.193e-23

Figure 3 shows the spot diagram of the designed system for 6 different positions in a field of view that covers an area of 50×50 cm². In this system, the aberrations were corrected using the optimization program in ZEMAX, and the root mean square size of the spot at

the end of the field of view was approximately 3 mm. The image quality curves of the spot diagram, focused energy, and MTF (MTF describes the transfer of modulation from the object to the image as a function of spatial frequency and commonly used to specify lens performance, and as an optimization and tolerancing target during lens design) as well as their analysis indicate that the designed system has a high image quality.

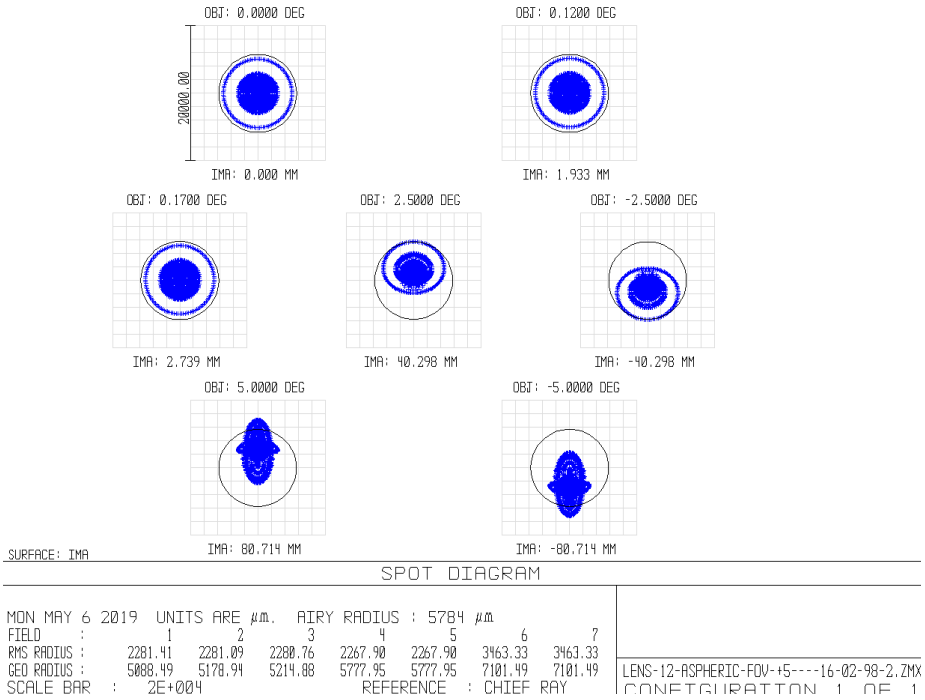

Fig. 3: Spot diagram of the designed aspherical lens in ZEMAX consisting of RMS radius and geometrical radius at 7 different positions in the field of view (0, 0.12, 0.17, 2.5, -2.5, 5, and -5 degrees).

2-2- Fresnel lens

A zone plate is a tool for image formation whose mechanism is not refraction, but rather diffraction in the aperture rings. The interference of the diffracted radiation generates the image. The spherical wave-front can be modified by using materials with different permittivities (Fig. 4.(a)) or phase correction areas (Fig. 4.(b)) [28,35].

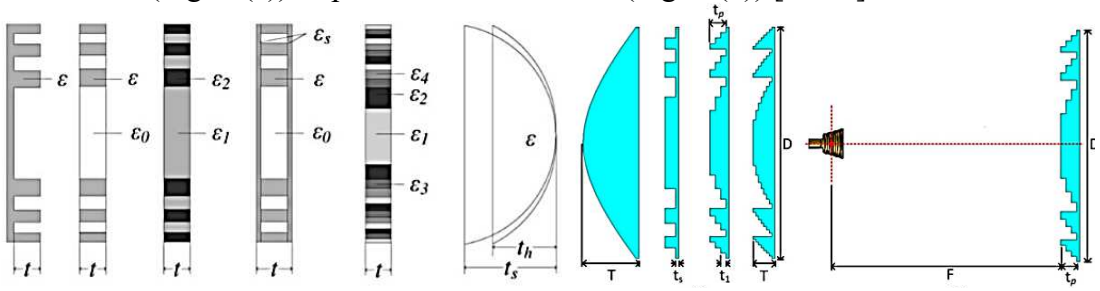

Fig. 4: Example of a Fresnel lens: (a) Multi-dielectric Fresnel zone plate lens, and (b) grooved Fresnel zone plate lens (where ε is the relative permittivity of the material and t is its thickness in different steps of designing) [28,35].

When the wave-front passes through the lens, the lens imposes a phase difference on the wave. The result is nearly a spherical wave-front that converges on the focal point of the lens [36]. By applying simple rules during the design process, a Fresnel lens antenna can achieve high efficiency with low side lobe levels. In a grooved Fresnel Zone plate lens, for having acceptable complexity, phase transfer steps can be used when the phase change reaches the half phase, quarter phase, and p phase. Therefore, each time the phase change reaches 180, 90, and 2π/p, the Fresnel lens compensates the phase. The parameter p corresponds to the number of compensations made during a 360-degree phase change. Since this compensation is not complete, the lens will have limited efficiency [37-39]. In a Fresnel lens, each groove forms a prism, so the Fresnel lens is made up of a set of prisms. The grooves near the center of the Fresnel lens are almost flat and shallow, and the grooves near the outside points have deep and sharp angles [40-42].
All diffraction areas contribute to focusing the light at the right point. For the design of the diffraction lens, the transition points should be calculated for each area, which is a correct multiple of the wavelength relative to the focal point of the lens (Fig. 5 [36]).

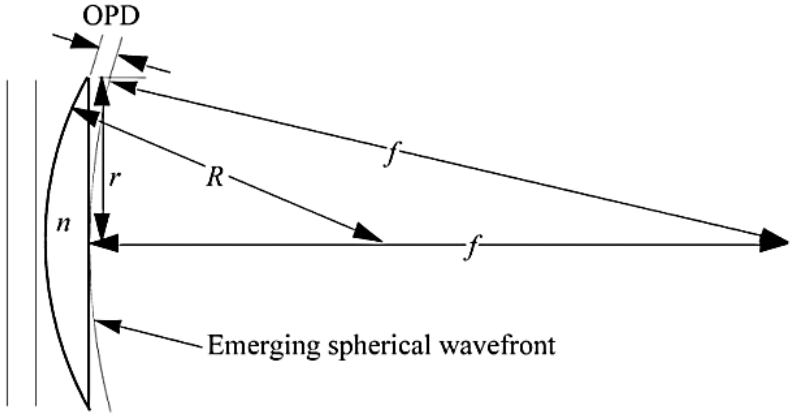

Fig. 5: Geometry used to determine the locations of transition points for a diffraction lens. OPD denotes the optical path difference, r is the semi-diameter, R is the radius, f is focal length and n is the refractive index of the lens.

In a lens with the focal length f, which operates at wavelength λ (for 2π phase, the change is equal to one λ of the optical path difference), the radius of the area p, where the phase change is equal to 2π, can be obtained as follows using Pythagorean theorem:

$$r_p^2 = 2fp\lambda \quad (4)$$

The phase difference caused by the lens is the difference between the input wave at any point and the phase delay due to passing through the lens at distance r from the axis, which is given as follows:

$$\Delta\varphi(r) = 2\pi(n-1)r^2/2R\lambda \quad (5)$$

The optical path difference at different points of the wave-front can be written as follows:

$$OPD = \Delta\varphi(r)\lambda/2\pi \quad (6)$$

ZEMAX calculates the location of the transition points for a symmetric lens phase profile (even powers of radius) by minimizing the aberrations. The phase function in this program is as follows:

$$\varphi(r) = 2\pi/\lambda\, OPD = 2\pi/\lambda\ (A_1 r^2 + A_2 r^4 + A_3 r^6 + A_4 r^8) \quad (7)$$

The Fresnel lens substrate that is designed by ZEMAX is a flat disk. Its profile is made of radial flat surfaces whose endpoints are defined by SAG expression [36].

The two-dimensional design of the Fresnel lens is illustrated in Fig. 6. Its input aperture has a radius of 330 mm, and there are 16 grooves in this Fresnel lens. The central thickness of the designed Fresnel lens is 12.7 mm. Additionally, the spherical surface radius of this lens is 778.9 mm and its conical coefficient is equal to -1.115.

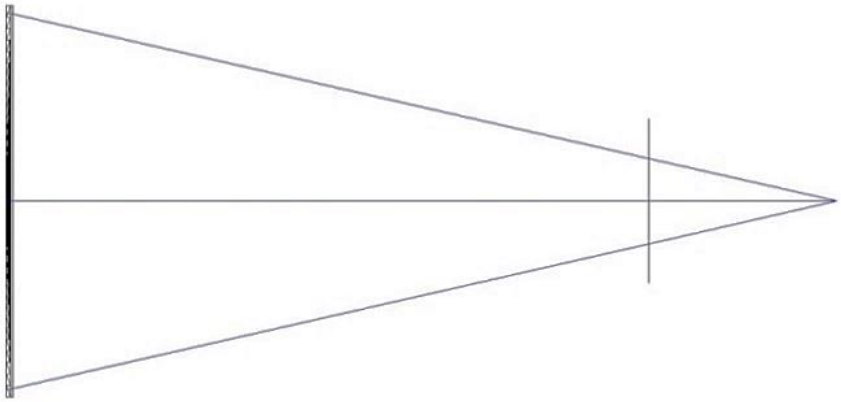

Fig. 6: The schematic drawing of Fresnel lens with a diameter of 660 mm and a thickness of 12.7 mm at a central frequency of 94 GHz in ZEMAX.

For designing this type of lens in ZEMAX, the non-sequential component of Fresnel was used and its 3D design is shown in Fig. 7. This lens weighs 4.5 kg, which is considerably lower compared to the corresponding spherical and aspherical lenses. This design can be used in a low-weight millimeter wave imaging system with a resolution of 30 mm at a distance of 5 m.

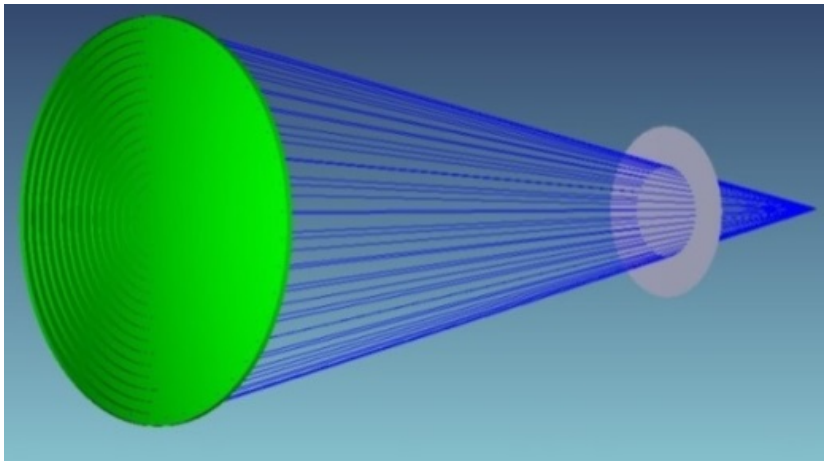

Fig. 7: Three dimensional design of the Fresnel lens with HDPE at 94 GHz in ZEMAX. The energy is converged at the focal point.

Figure 8 shows the optimized Fresnel lens spot diagram. The intensity profile of the image spot contains a central lobe and several side lobes with gradually decreasing intensity containing 84% received energy of the target. The RMS of the lens spot's radius is 5.626 mm. To optimize the lens, the image plane is set as the global coordinate

reference, and the default merit function is used with RMS of the spot's radius of all configurations as the convergence criteria.

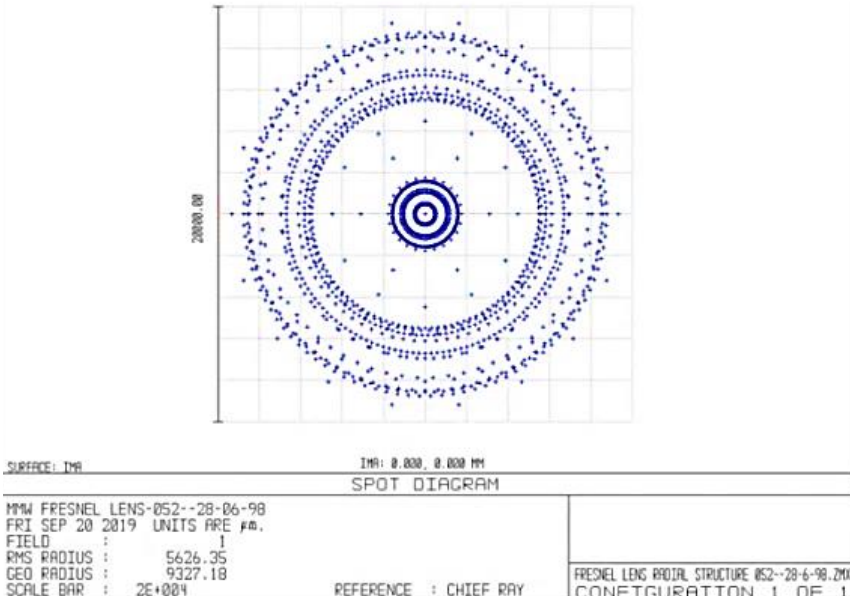

Fig. 8: Optimized Fresnel lens spot diagram with an RMS radius of 5.626 mm.

2-3- Design and simulation of secondary optics

For the design of the secondary optics, one should specify the horn profile and its wall type (flat or corrugated). It is very important to match the feed horn beam width to the system F-number (F#) to optimize the performance of the system. The usual values of the optimum feed taper (a measure of the ratio of the power reduction at the opening edge to the power on the axis) range from -10 to -13 dB (Fig. 9). If $\theta_{-10dB} \gg \theta_0$, spillover loss will occur and some power will be lost. If $\theta_{-10dB} \ll \theta_0$, the amplitude taper loss and phase error loss result in deviations from amplitude and constant phase in the opening field [43].

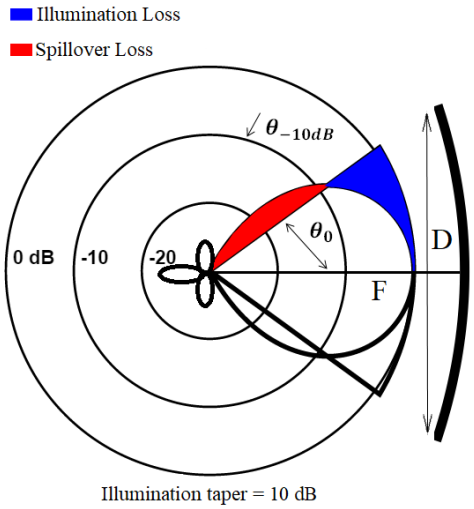

Fig. 9: Spillover loss of the combined lens and horn antenna. θ_0 is the opening angle of the lens, θ_{-10dB} is the angle for -10 dB illumination taper, F is the focal length and D is the lens diameter.

The performance of the horn antenna with a linear opening wall is improved by profiling the wall [43]. Horn profile can be sinusoidal, tangential, exponential, hyperbolic, polynomial, etc. [44]. The Gaussian profiled horn antenna provides a smooth transition from the waveguide to the flare, which improves the matching between the antenna and free space. This improved matching ensures a better radiation pattern and more bandwidth and increases the total efficiency of the system [45]. Horn antennas with Gaussian profile can be used to optimize various parameters, such as beam diffraction, bandwidth, side lobe levels, transverse polarization, orientation, gain, and efficiency. In Gaussian horn antennas, the main features of the radiation pattern of conical horn antenna are preserved. Furthermore, side lobe levels and cross-polarization surface are significantly reduced [45, 46].

The next step after selecting the wall profile of the horn is choosing the feature of the wall (flat or corrugated). Flat-wall horn antennas have some problems that can be resolved by wall corrugation. These problems include uneven beam widths, uneven phase centers in two orthogonal planes, more side lobes on E-plane than H-plane, and diffraction from E-plane walls that will cause back lobes [18].

First, we designed an optimized Gaussian profile horn with a flat wall in FEKO software for feeding the desired optical system. The structure of this horn is shown in Fig. 10.

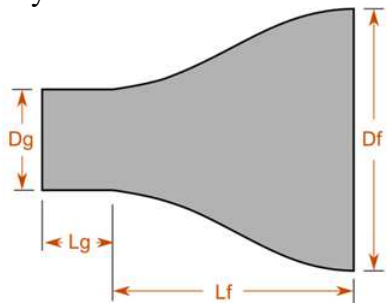

Fig. 10: Schematic of the designed Gaussian profile horn with flat wall, where Dg, Lg, Df, and Lf are the waveguide diameter, waveguide length, final diameter of the Gaussian profile, and profile length, respectively.

The optimized parameters of the horn are listed in Table 2, where Dg is the waveguide diameter, Lg is the waveguide length, Df is the final diameter of the Gaussian profile and Lf is the profile length.

Table 2: Optimized parameters of Gaussian profile horn.

Dg	Lg	Df	Lf
16.43	19.14	3.18	2.55

Figure 11 shows the radiation patterns of the flat wall Gaussian horn at 94 GHz in two orthogonal planes.

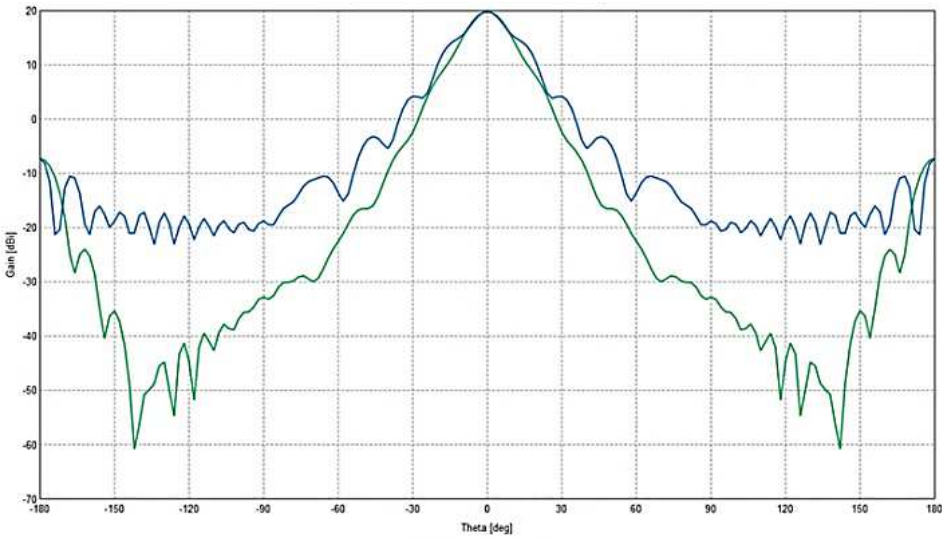

Fig. 11: Radiation patterns of flat wall Gaussian profile horn at 94 GHz, in E (green line) and H (blue line) planes.

Then, we designed a Gaussian profile horn with a corrugated wall and reduced side lobes. Side lobes allow receiving radiation from unwanted directions. Moreover, the symmetry of patterns means less aberrations, so more focused energy with lower reflection can be transferred from the aperture to the detector. The horn is well designed to match the primary optics.

2-4- Designing corrugated Gaussian feeding horn

The structure of this horn was designed according to the instructions in Ref. [47], and the obtained parameters were optimized in FEKO. This horn comprises a circular waveguide with a transition from a flat linear section to a corrugated linear section, which is used as a mode converter (Fig. 12). The depth of the grooves in the conical convertor section starts with an initial value of approximately half the wavelength at the maximum frequency and ends with one quarter of the wavelength at the central frequency.

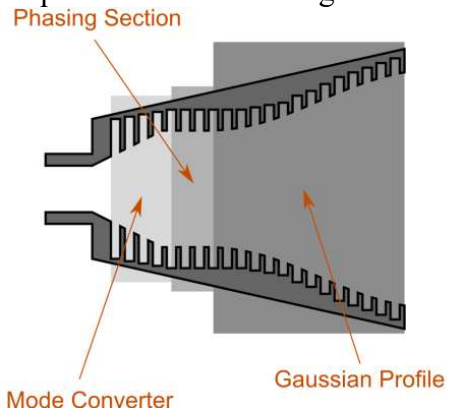

Fig. 12: Schematic of the corrugated Gaussian horn.

The mode converter is a phasing section that feeds the Gaussian profile section. The depths of all slots after the converter are equal. These sections are described below.

2-4-1 Mode converter

The Gaussian horn antenna has to be fed by a purely HE_{11} mode. Therefore, in the horn neck region, an impedance converter was used to accommodate flat single-mode waveguide TE_{11} with the corrugated waveguide [48]. This mode converter usually starts with a single-mode circular flat propagator waveguide TE_{11} and terminates in the opening diameter required for the phasing section, which feeds the Gaussian profile of the horn antenna. The parameters proposed for the corrugated conical horn (Fig. 13) are listed in Table 3.

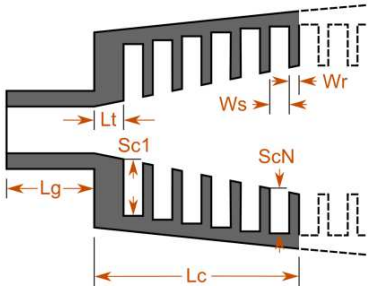

Fig. 13: Mode converter with values optimized in FEKO.

In Table 3, 2a is the waveguide diameter, Lg is the waveguide length, and Lt is the transition region length; Sc1 and ScN are the depths of the first and last grooves in the converter; Ws is the groove width, Wr is the ridge width, Lc is the axial length in the converter section, and Nc is the number of grooves in the converter section.

Table 3: Mode converter parameters (mm).

2a	Lg	Lt	Sc1	ScN	Ws	Wr	Lc	Nc
2.55	3.18	0.797	1.27	0.79	0.53	0.13	8.23	10

2-4-2 Phasing section

Due to the compression of the corrugated horn antenna in the first section, the directivity is low and the phase centers on E and H planes do not match. Therefore, a phasing section is used to overlap the phase centers in the desired frequency band. This section also improves the combination of TE_{11} and TM_{11} modes. The phasing section is shown in Fig. 14 and its design parameters are given in Table 4.

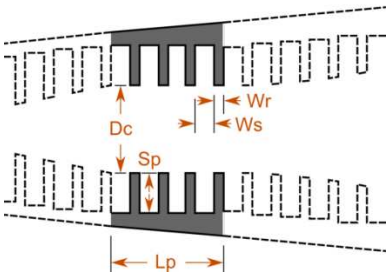

Fig. 14: Phasing section in FEKO.

In Table 4, Dc is the phasing section diameter, Sp is the groove depth in the phasing section, Lp is the length of the phasing section, and Np is the number of grooves in the phasing section; Ws and Wr are the groove and ridge widths, respectively.

Table 4: Phasing section parameters (mm).

Dc	Sp	Lp	Np
9.17	0.79	2.65	4

2-4-3 Gaussian section parameters

The values of the design parameters in the Gaussian section (Fig. 15) are given in Table 5.

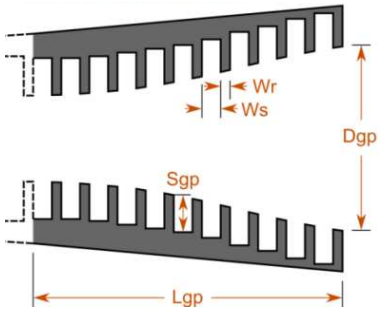

Fig. 15: Corrugated Gaussian section in FEKO at 94 GHz.

In Table 5, Dgp is the final diameter of the Gaussian profile, Sgp is the Gaussian profile depth, Lgp is the Gaussian profile length, and Ngp is the number of grooves in the Gaussian profile section; Ws and Wr are the groove and ridge widths, respectively.

Table 5: Gaussian section parameters (mm).

Dgp	Sgp	Lgp	Ngp
13.9	0.79	9.96	15

3-1-4- Simulation results of Gaussian corrugated horn

The most important parameters in our design are the symmetry of the radiation pattern and low side lobe level. Figure 16 shows the 3D radiation pattern of the designed horn, which has a gain of about 20 dBi. Moreover, the designed horn has a very symmetrical pattern in both orthogonal planes and the side lobes are reduced to a large extent compared to other conventional horns in this wavelength range.

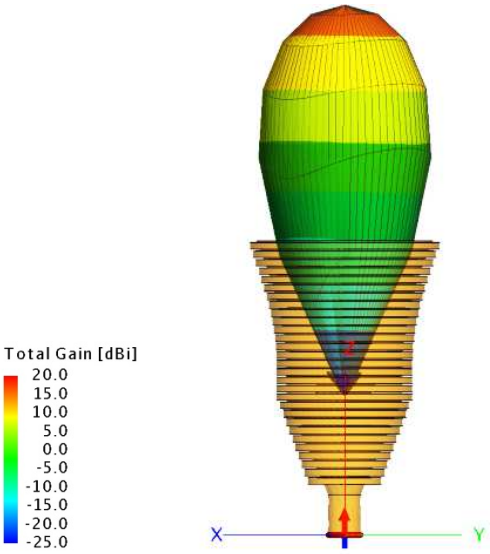

Fig. 16: Radiation pattern of the designed corrugated Gaussian horn at 94 GHz.

Figure 17 shows the radiation pattern of the corrugated horn at the desired design frequency in E and H planes. At the optimal frequency band, the side lobes levels are below -38.5 dB, which is a very good result.

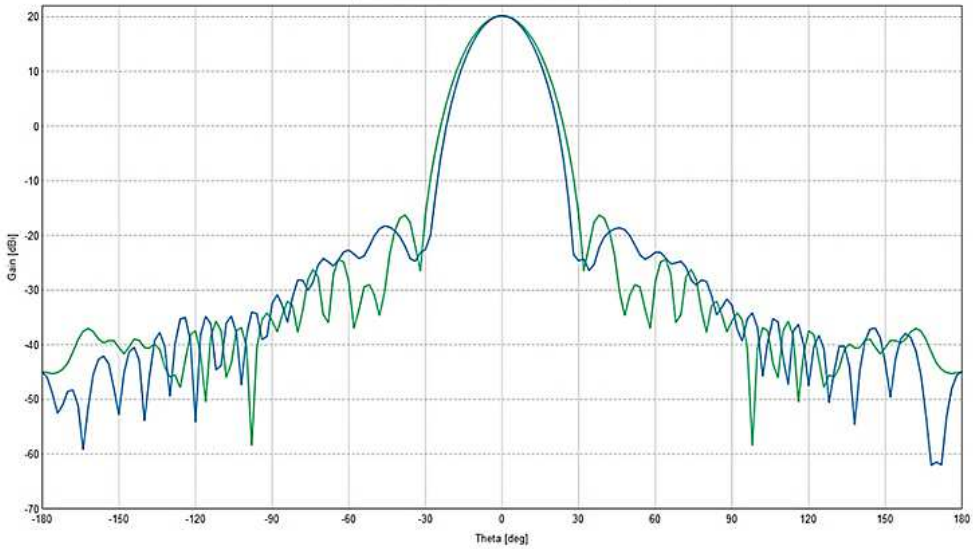

Fig. 17: Far-field radiation pattern at 94 GHz in E (green line) and H (blue line) planes.

The pattern symmetry is very good and the horn -10 dB beamwidth is about 40 degrees, which makes it appropriate for quasi-optical transition systems.

3- Conclusion

In this study, we designed and simulated a millimeter wave imaging system, which included a lens and a feedhorn. With a lens aperture diameter of 65 cm, the system was capable of imaging an object with a resolution of 30 mm in a 5-meter imaging range at a central frequency of 94 GHz. The aspherical lens, which was designed for the millimeter

wave camera, yielded a high-quality system with well-corrected aberrations. The image quality curves also showed the high quality of the designed system. In addition, to reduce the weight and volume of the imaging system, a Fresnel lens was designed and simulated in this wavelength band. An optimized corrugated Gaussian horn was designed with a gain of about 20 dB and a 10-dB beamwidth of 40° in E and H planes to obtain proper axially symmetric patterns. According to the analytical and simulation results, it was concluded that the combination of a Fresnel lens and Gaussian corrugated horn is very advantageous and this complete quasi-optical system can be used in high-resolution millimeter wave imaging to detect hidden objects in security imaging applications.

Availability of data and materials:

'Not applicable'.

Competing interests:

'The authors declare that they have no competing interests'.

Funding:

'Not applicable'.

Authors' contributions:

Faeze Jadidi carried out the initial studies, designed the optical system and horn, and drafted the manuscript. Abdollah Eslamimajd participated in the design of the study and performed the statistical analysis. Alireza Erfaniyan and Seyed Hossein Mohseni Armaki conceived of the study, participated in its design, and helped to draft the manuscript. All authors read and approved the final manuscript.

Acknowledgments:

'Not applicable'.

Endnotes:

'Not applicable'.

Reference

1. Chen, C, Prather, DW, Siegel, PH: Design of a 600 GHz fresnel lens antenna for passive and active imaging, In: 2007 IEEE Antennas and Propagation Society International Symposium, 4385-4388, Honolulu, HI, USA (2007).

2. Zhou, J, Chen, Q, Zhang, Y, Fan, Y, Da Xu, K: Aspheric dielectric lens antenna for millimeter-wave imaging system. In:Asia-Pacific Microwave Conference (APMC), 3, 1-3, IEEE, Nanjing, China (2015). doi:10.1109/APMC.2015.7413384.
3. Sheen, DM, McMakin, DL, Hall, TE: Three-dimensional millimeter-wave imaging for concealed weapon detection, IEEE Trans. Microw. Theory Tech. 49, 1581-1592 (2001). doi:10.1109/22.942570
4. Zhang, C, Deng, C: Passive terahertz imager. In 2011 International Conference on Infrared, Millimeter, and Terahertz Waves, IEEE, Houston, TX, USA (2011). doi: 10.1109/irmmw-THz.2011.6105113
5. Clark, SE, Lovberg, JA, Martin, CA, Kolinko, VG: Passive millimeter-wave imaging for airborne and security applications, Proc. SPIE 5077, Passive Millimeter-Wave Imaging Technology VI and Radar Sensor Technology VII, (2003). https://doi.org/10.1117/12.484871
6. Lettington, A, Alexander, N, Dunn, D: A new opto-mechanical scanner for millimeter and sub-millimeter wave imaging, in Passive Millimeter-Wave Imaging Technology VIII, 5789, 16-24, SPIE, Orlando, Florida, United States (2005). https://doi.org/10.1117/12.597745.
7. Sheen, DM, McMakin, DL, Hall, TE: Near field imaging at microwave and millimeter wave frequencies. In: 2007 IEEE/MTT-S International Microwave Symposium, 1693-1696, IEEE, Honolulu, HI, USA (2007). doi: 10.1109/MWSYM.2007.380033
8. Kim, WG, Moon, NW, Singh, MK, Kim, HK, Kim, YH: Characteristic analysis of aspheric quasi-optical lens antenna in millimeter-wave radiometer imaging system, Appl. Opt. 52, 1122-1131 (2013). doi: 10.1364/AO.52.001122
9. Wiltse, JC: History of millimeter and submillimeter waves, IEEE Trans. Microw. Theory Tech. 32, 1118-1127 (1984). doi:10.1109/TMTT.1984.1132823
10. Giles, DA, Linfield Edmund, H, Pepper, M, Appleby, R:Passive millimetre–wave imaging and how it differs from terahertz imaging, Phil. Trans. R. Soc. A.362379–393 (2004). https://doi.org/10.1098/rsta.2003.1323
11. Appleby, R, Anderton, RN: Millimeter-wave and submillimeter-wave imaging for security and surveillance, Proceedings of the IEEE, 95(8), 1683-1690 (2007). doi: 10.1109/JPROC.2007.898832.
12. Fischer, RE, Tadic-Galeb, B, Yoder, PR, Galeb, R, Kress, BC, McClain, SC, et al., Optical system design, 2 edition, McGraw-Hill Education (2008).
13. Diallo, AO, Czarny, R, Loiseaux, B, Holé, S: Comparison between a thin lens antenna made of structured dielectric material and conventional lens antennas, in Q-Band in a compact volume. IEEE Antennas and Wireless Propagation Letters 17(2), 307-310 (2017).
14. Minin, IV, Minin, OV: Basic principles of Fresnel antenna arrays, 19, Springer Science & Business Media (2008).
15. O'Sullivan, CM, Murphy, JA: Field guide to terahertz sources, detectors, and optics, SPIE (2012). https://doi.org/10.1117/3.952851
16. Jinghui, Q, Zhong, Z, Kai, L, Gaofei, L, Fei, X: Design and measurement of quasi-optics for millimeter wave imaging system, 2009 IEEE International Workshop

on Imaging Systems and Techniques, Shenzhen, 2009, 132-135, doi:10.1109/IST.2009.5071618.
17. Walsby, E, Wang, S, Xu, J, Yuan, T, Blaikie, R, Durbin, S: Multilevel silicon diffractive optics for terahertz waves, J. Vac. Sci. Technol B. 20, 2780-2783, (2002). doi:10.1116/1.1518021
18. Milligan, TA: Modern antenna design, 2 edition, Wiley-IEEE Press (2005).
19. Henselmans, R: Non-contact measurement machine for freeform optics, Technische Universiteit Eindhoven, Citeseer (2009).
20. Chen, Q, Fan, Y, Zhou, J, Song, K: Design of Quasi-Optical Lens Antenna for W-Band Short Range Passive Millimeter-Wave Imaging, J. Comput. Commun. 3, p. 93, (2015). doi: 10.4236/jcc.2015.33016.
21. Yeom, S, Lee, DS, Son, JY, Jung, MK, Jang, Y, Jung, SW: Real-time outdoor concealed-object detection with passive millimeter wave imaging, Opt. Express. 19, 2530-2536 (2011). doi: 10.1364/OE.19.002530.
22. Li, CM, Huang, CY, Chang, LY, Yu, YC, Nien, CC, Tarng, JH: Development of a compact total power passive millimeter-wave imaging system, in 2011 IEEE International Symposium on Radio-Frequency Integration Technology, 153-156, Beijing, China (2011). doi**:** 10.1109/RFIT.2011.6141793
23. Garrett, JE, Wiltse, JC: Fresnel zone plate antennas at millimeter wavelengths, Int. J. Infrared Mill. 12, 195-220 (1991).
24. Keshavarz, A, Soltanzadeh, MJ: Designing the optimal Fresnel lenses by using Zemax software, J. optoelectron. nanostructures. 3, 87-96 (2018).
25. Rodríguez, J, Hristov, HD, Grote, W: Fresnel zone plate and ordinary lens antennas: Comparative study at microwave and terahertz frequencies, In: 2011 41st European Microwave Conference, 894-897, IEEE, Manchester, UK (2011).
26. León Fernández, GL, Herrán Ontañón, F, Munoz, M, Las Heras Andrés, FL, Hao, Y: Millimeter-wave offset Fresnel zone plate lenses characterization, Prog. Electromagn. Res. C. 54, 125-131 (2014).
27. Jouadé, A: Millimeter-wave radar imaging systems: focusing antennas, passive compressive devicefor MIMO configurations and high resolution signal processing, Ph.D. Thesis, University of Rennes (2017).
28. Sleiman, J: Terahertz Imaging and Spectroscopy: Application to Defense and Security in front of the examination panel, Ph.D. Thesis, University of Bordeaux (2016)
29. Luukanen, A, Appleby, R, Kemp, M, Salmon, N: Millimeter-wave and terahertz imaging in security applications. In: Terahertz Spectroscopy and Imaging, 491-520. Springer, (2012).
30. Kerdemelidis, V, James, GL, Smith, BA: Some methods of reducing the sidelobe radiation of existing reflector and horn antennas, In: Recent Advances in Electromagnetic Theory, 235-251, Springer (1990).
31. Ibrahim, DGA: Enhancement of the steepness measurement of a film thickness edge using wavelet transforms with fringe thinning, OSA Continuum 3(7), 1930-1939 (2020).
32. Ibrahim, DGA: Demodulation of a parabolic interferogram in time domain for rough surface characterization, Applied Physics B, 126(9), 1-7 (2020).

33. Murphy, JA, Trappe, N, Withington, S: Gaussian beam mode analysis of partial reflections in simple quasi-optical systems fed by horn antennas. Infrared physics & technology 44(4), 289-297 (2003). https://doi.org/10.1016/S1350-4495(03)00127-0
34. Gundersen, J, Wollack, E: Millimeter wave corrugated platelet feeds. In: Journal of Physics: Conf. Ser 2009.
35. Hristov, HD, Rodriguez, JM: Design equation for multidielectric Fresnel zone plate lens. IEEE Microwave and Wireless Components Letters 22(11), 574-576 (2012). doi: 10.1109/LMWC.2012.2224099
36. O'Shea, DC, Suleski, TJ, Kathman, AD, Prather, DW:Diffractive optics: design, fabrication, and test, 62, SPIE press (2004) https://doi.org/10.1117/3.527861.
37. Black, DN, Wiltse, JC: Millimeter-wave characteristics of phasecorrecting Fresnel zone plates. IEEE Transactions on Microwave Theory and Techniques, 35(12):1122–1129, (1987). doi:10.1109/TMTT.1987.1133826
38. Hristov, HD, HAJ Herben, M: Millimeter-wave Fresnel-zone plate lens and antenna. IEEE Transactions on Microwave Theory and Techniques, 43(12):2779–2785, (1995).
39. Jouade, A, Bor, J, Himdi, M, Lafond, O: Millimeter-wave fresnel zone plate lens with new technological process. International Journal of Microwave and Wireless Technologies, 1–6, 008 (2016). doi: https://doi.org/10.1017/S1759078716000854
40. Miller, O, McLeod, J, Sherwood, W: Thin sheet plastic Fresnel lenses of high aperture, J. Opt. Soc. Am. 41(11), 807-815 (1951). https://doi.org/10.1364/JOSA.41.000807
41. Davis, A, Kühnlenz, F:Optical design using Fresnel lenses: Basic principles and some practical examples, Opt. Photon. 2, 52-55 (2007).
42. Erismann, F:Design of a plastic aspheric Fresnel lens with a spherical shape, Opt. Eng. 36, 988-992 (1997).
43. Volakis, JL: Antenna engineering handbook (4th ed.). New York: McGraw-Hill (2007).
44. Granet, C:Profile options for feed horn design, in 2000 Asia-Pacific Microwave Conference. Proceedings (Cat. No. 00TH8522), 1448-145, IEEE, Sydney, NSW, Australia (2000).
45. Kishk, A, Lim, CS:Comparative Analysis Between Conical and Gaussian Profiled Horn Antennas-Abstract, J. ELECTROMAGNET. WAVE. 17, 599-600 (2003).
46. De Miguel-Hernández, J, Hoyland, RJ: Fundamentals of horn antennas with low cross-polarization levels for radioastronomy and satellite communications. Journal of Instrumentation 14(08), R08001 (2019). doi:10.1088/1748-0221/14/08/R08001
47. Granet, C, James, GL:Design of corrugated horns: A primer, in IEEE Antennas and Propagation Magazine, vol. 47, no. 2, 76-84, (2005). doi: 10.1109/MAP.2005.1487785.
48. Salimi, T, Maghoul, A, Abbasid, AA: Design of a compact Gaussian profiled corrugated horn antenna for low sidelobe-level applications. International Journal of Computer Theory and Engineering, Optics Express Vol. 20, Issue 9, 9371-9381 (2012). https://doi.org/10.1364/OE.20.009371

List of abbreviations:
'Not applicable'.

Figure Captions:

Fig. 1. Quasi-optics configuration consisting of a lens and feeding horn.

Fig. 2: Overview of the designed aspherical lens, consisting object plane (left), lens and image plane (right). The colors show different positions of object plane in field of view of the designed lens.

Fig. 3: Spot diagram of the designed aspherical lens in ZEMAX consisting of RMS radius and geometrical radius at 7 different positions in the field of view (0, 0.12, 0.17, 2.5, -2.5, 5, and -5 degrees).

Fig. 4: Example of a Fresnel lens: (a) Multi-dielectric Fresnel zone plate lens, and (b) grooved Fresnel zone plate lens (where ε is the relative permittivity of the material and t is its thickness in different steps of designing).

Fig. 5: Geometry used to determine the locations of transition points for a diffraction lens. OPD denotes the optical path difference, r is the semi-diameter, R is the radius, f is focal length and n is the refractive index of the lens.

Fig. 6: The designed Fresnel lens with a diameter of 660 mm and a thickness of 12.7 mm at a central frequency of 94 GHz in ZEMAX.

Fig. 7: Three dimensional design of the Fresnel lens with HDPE at 94 GHz in ZEMAX. The energy is converged at the focal point.

Fig. 8: Optimized Fresnel lens spot diagram with an RMS radius of 5.626 mm.

Fig. 9: Spillover loss of the combined lens and horn antenna. θ0 is the opening angle of the lens, θ-10dB is the angle for -10 dB illumination taper, F is the focal length and D is the lens diameter.

Fig. 10: Schematic of the designed Gaussian profile horn with flat wall, where Dg, Lg, Df, and Lf are the waveguide diameter, waveguide length, final diameter of the Gaussian profile, and profile length, respectively.

Fig. 11: Radiation patterns of flat wall Gaussian profile horn at 94 GHz, in E (green line) and H (blue line) planes.

Fig. 12: Schematic of the corrugated Gaussian horn.

Fig. 13: Mode converter with values optimized in FEKO.

Fig. 14: Phasing section in FEKO.

Fig. 15: Corrugated Gaussian section in FEKO at 94 GHz.

Fig. 16: Radiation pattern of the designed corrugated Gaussian horn at 94 GHz.

Fig. 17: Far-field radiation pattern at 94 GHz in E (green line) and H (blue line) planes.

Figures

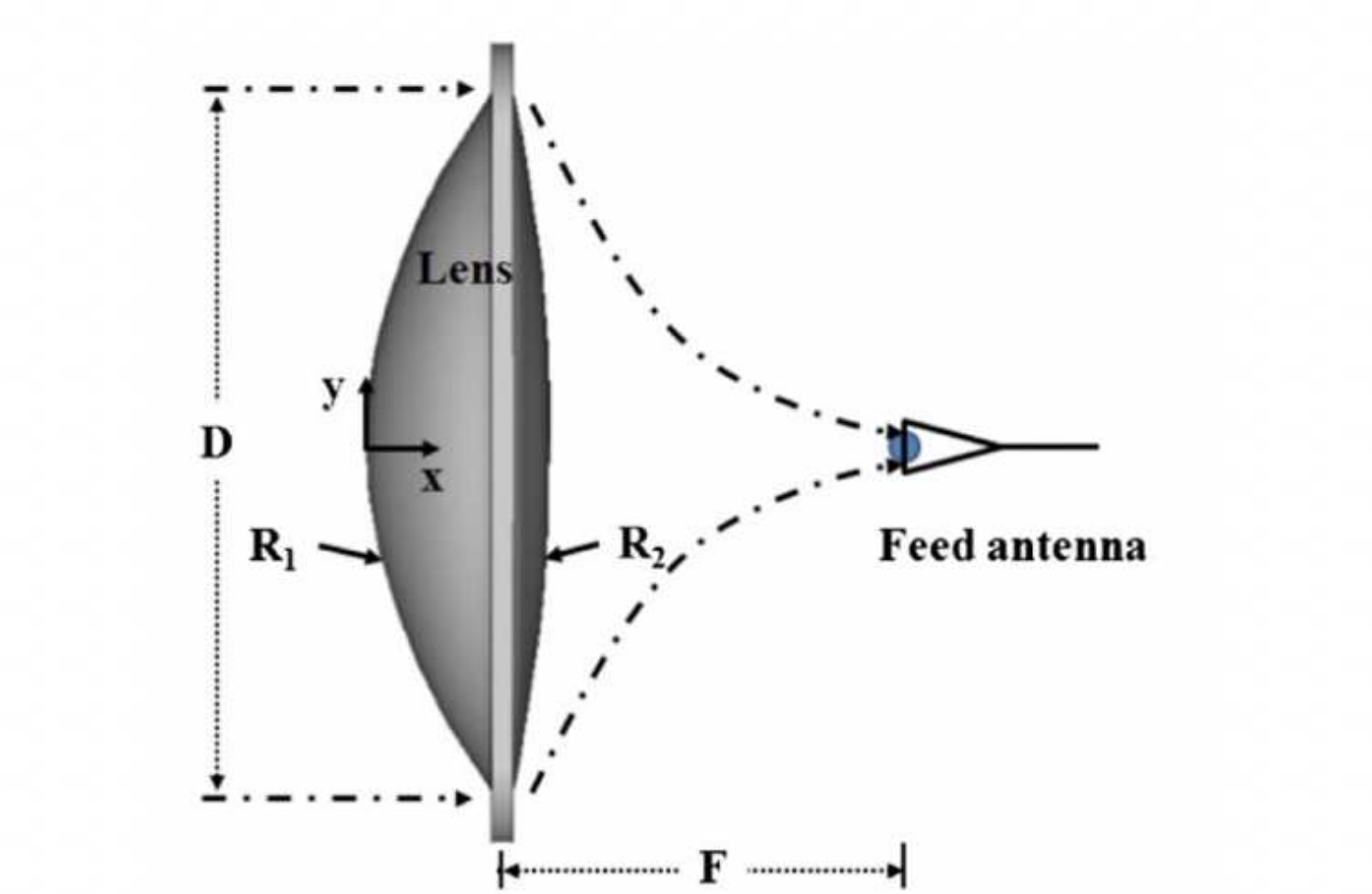

Figure 1

Quasi-optics configuration consisting of a lens and feeding horn.

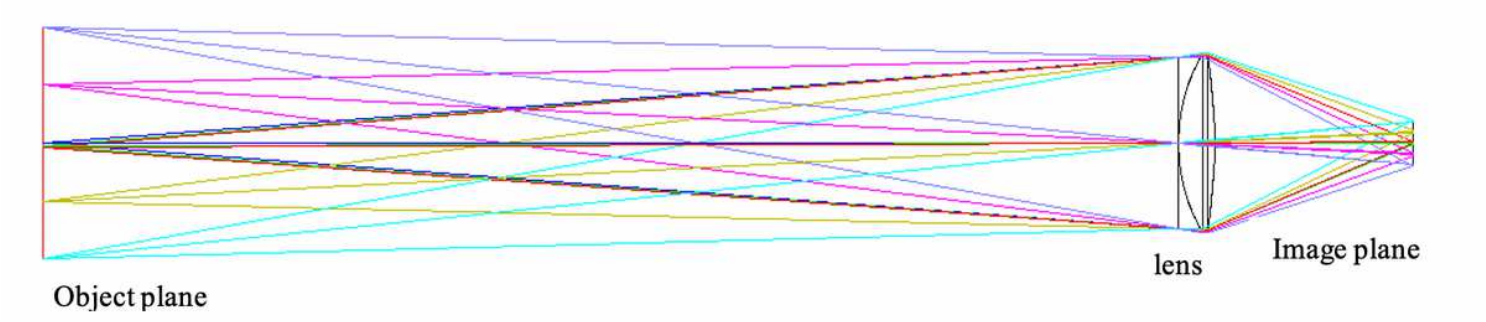

Figure 2

Overview of the designed aspherical lens, consisting object plane (left), lens and image plane (right). The colors show different positions of object plane in field of view of the designed lens.

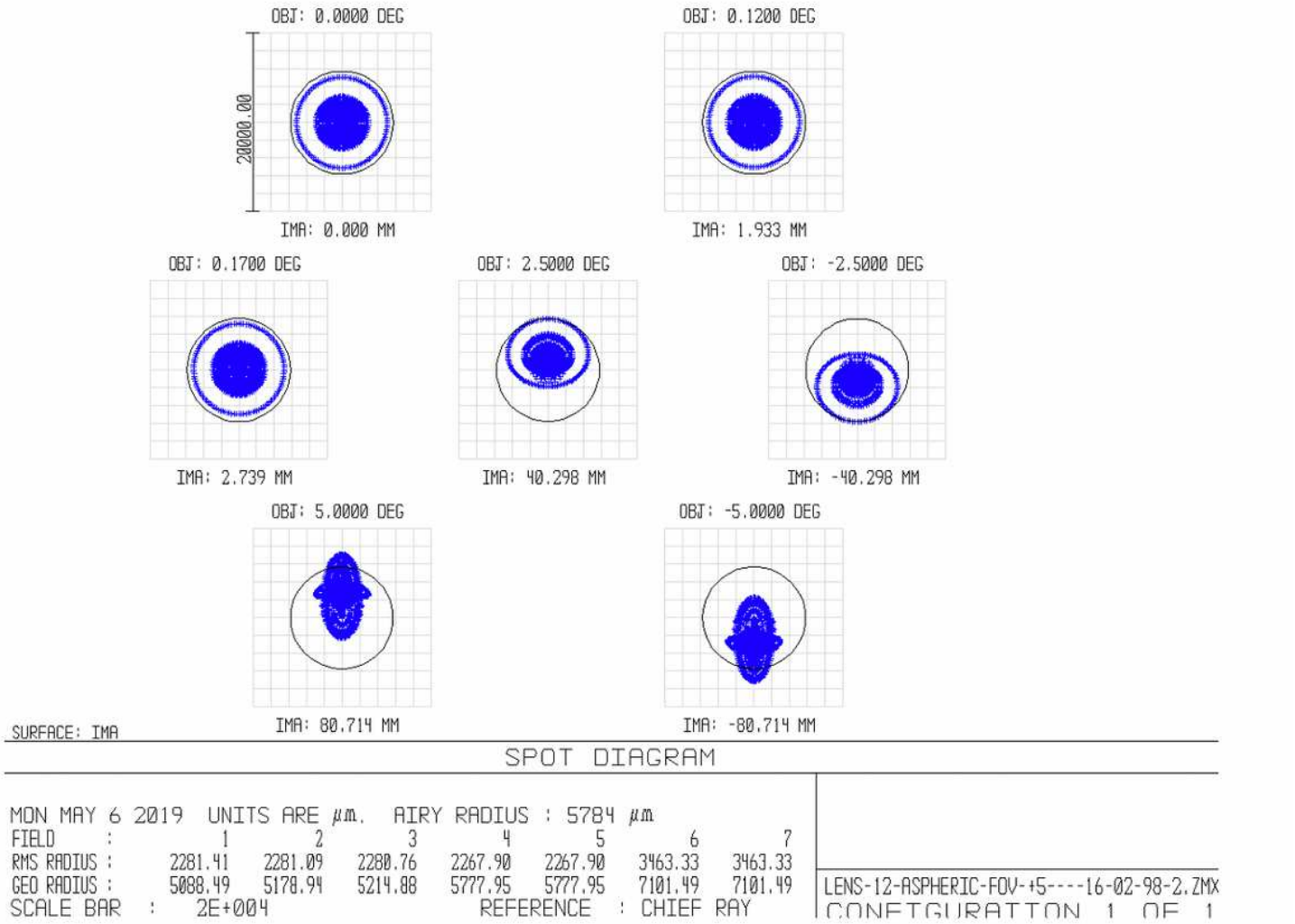

Figure 3

Spot diagram of the designed aspherical lens in ZEMAX consisting of RMS radius and geometrical radius at 7 different positions in the field of view (0, 0.12, 0.17, 2.5, -2.5, 5, and -5 degrees).

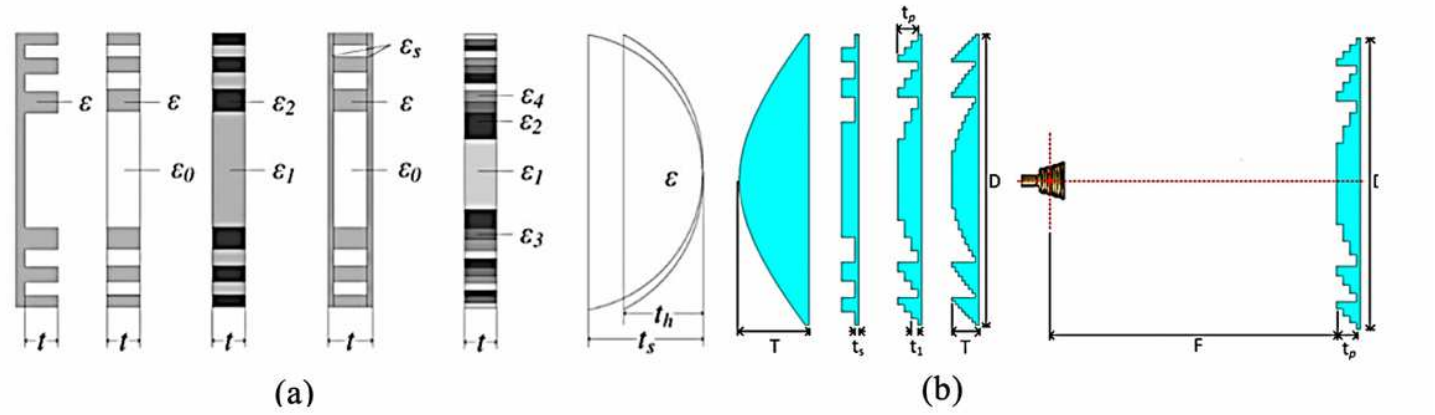

Figure 4

Example of a Fresnel lens: (a) Multi-dielectric Fresnel zone plate lens, and (b) grooved Fresnel zone plate lens (where ε is the relative permittivity of the material and t is its thickness in different steps of designing).

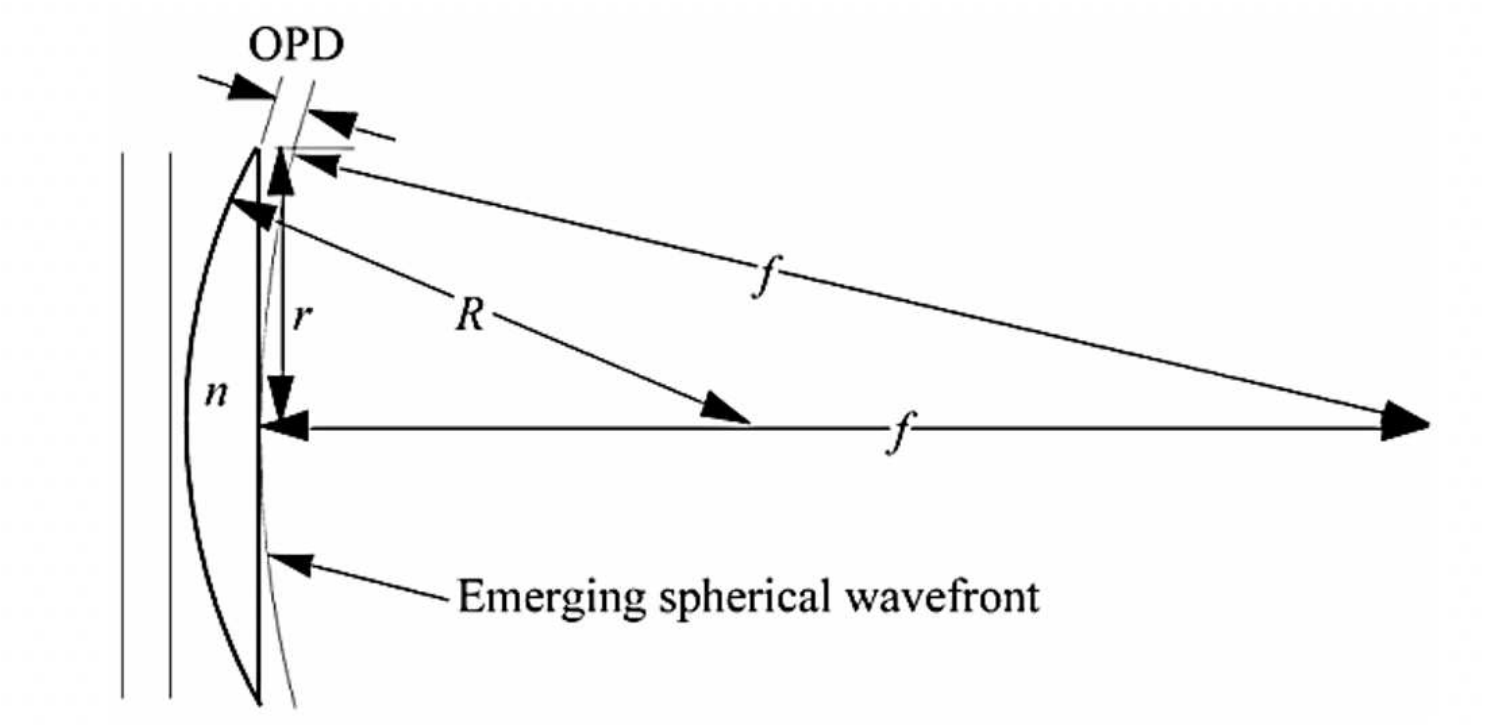

Figure 5

Geometry used to determine the locations of transition points for a diffraction lens. OPD denotes the optical path difference, r is the semi-diameter, R is the radius, f is focal length and n is the refractive index of the lens.

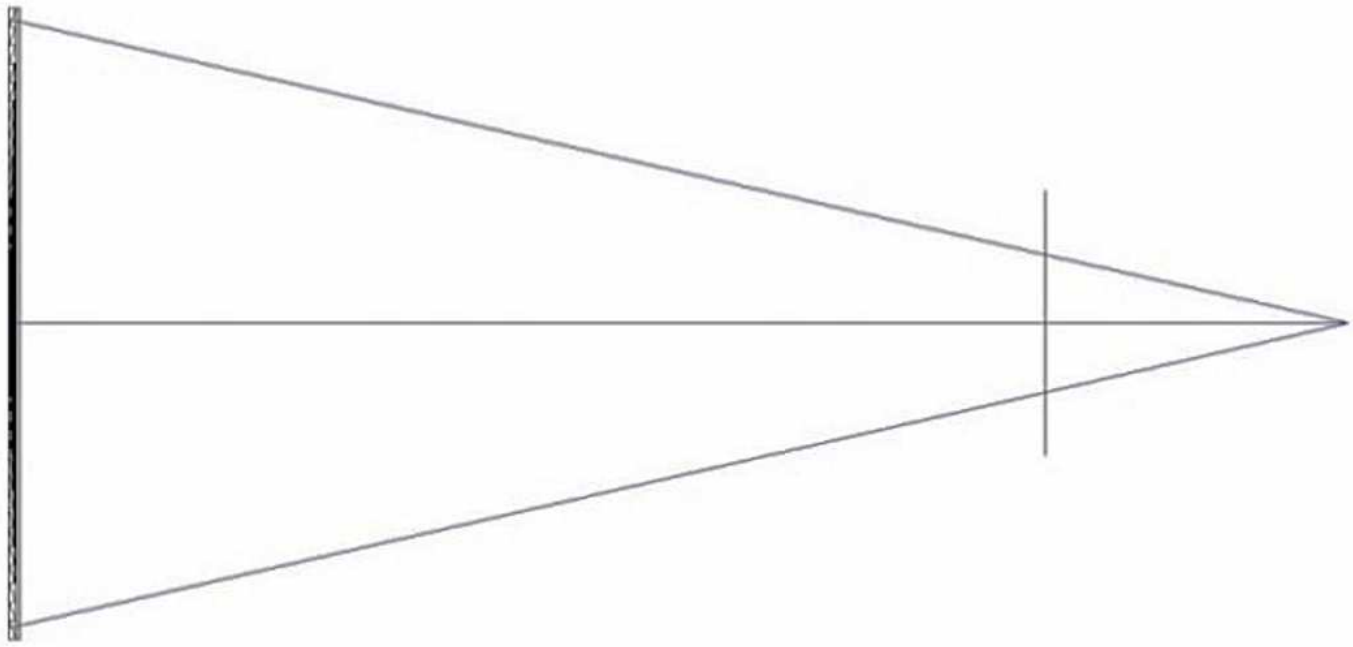

Figure 6

The designed Fresnel lens with a diameter of 660 mm and a thickness of 12.7 mm at a central frequency of 94 GHz in ZEMAX.

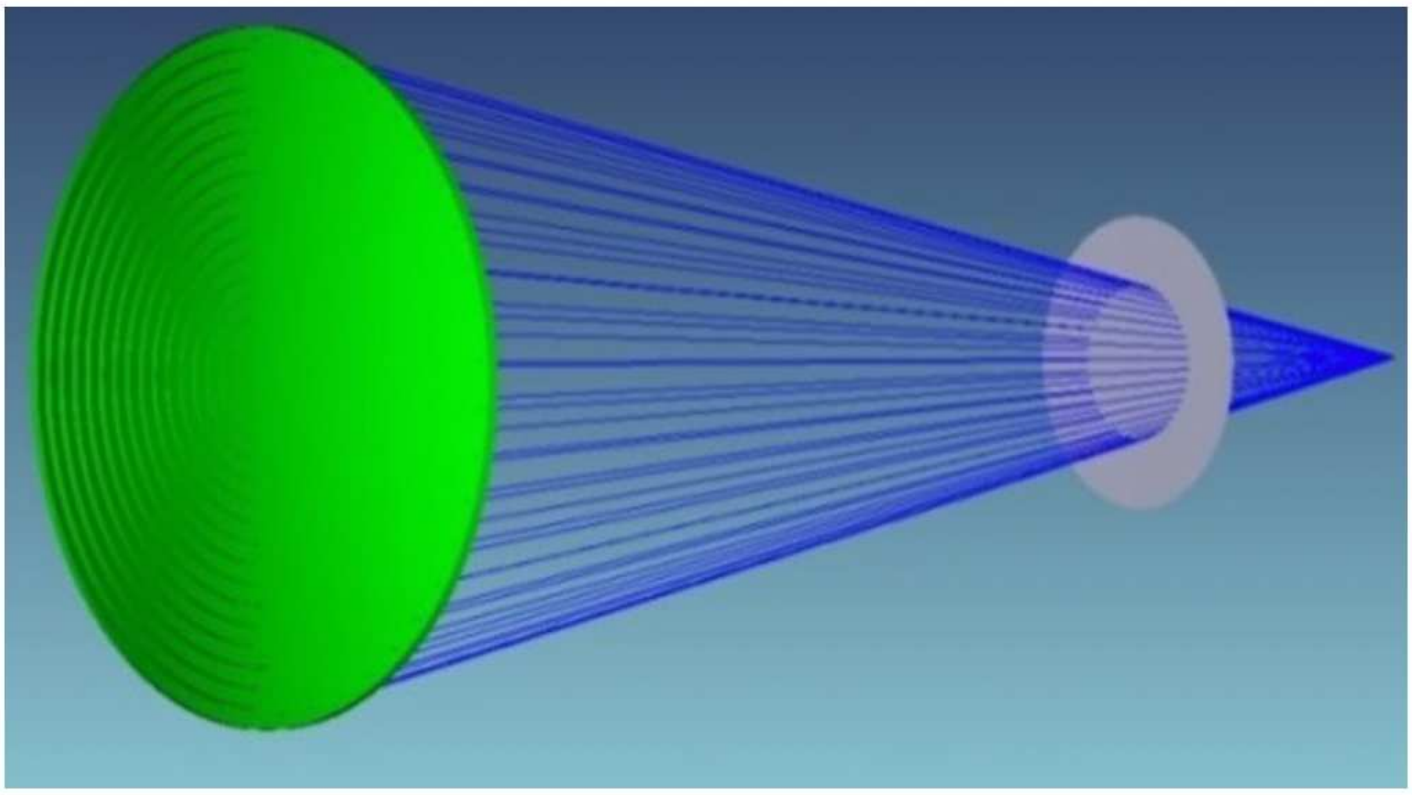

Figure 7

Three dimensional design of the Fresnel lens with HDPE at 94 GHz in ZEMAX. The energy is converged at the focal point.

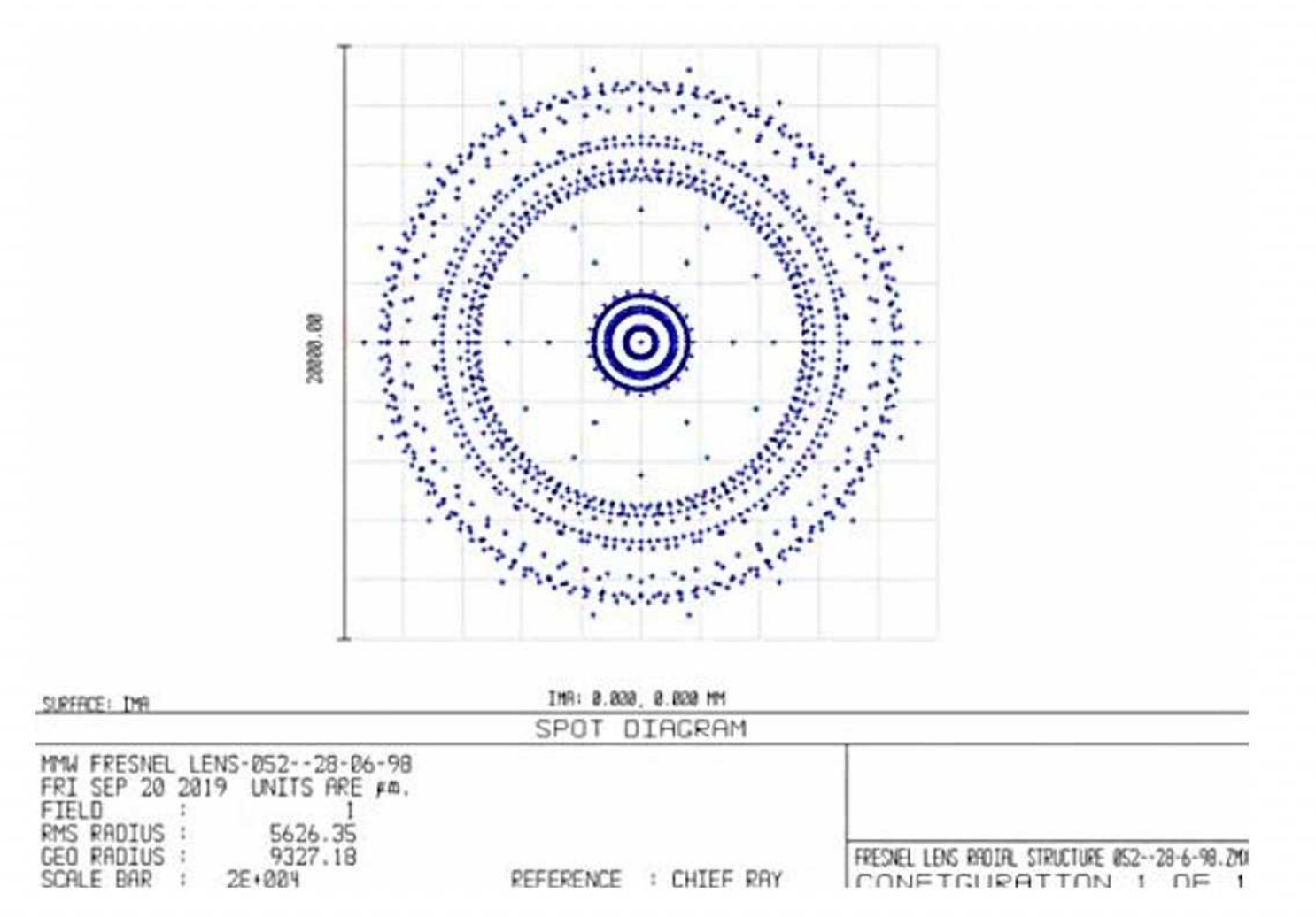

Figure 8

Optimized Fresnel lens spot diagram with an RMS radius of 5.626 mm.

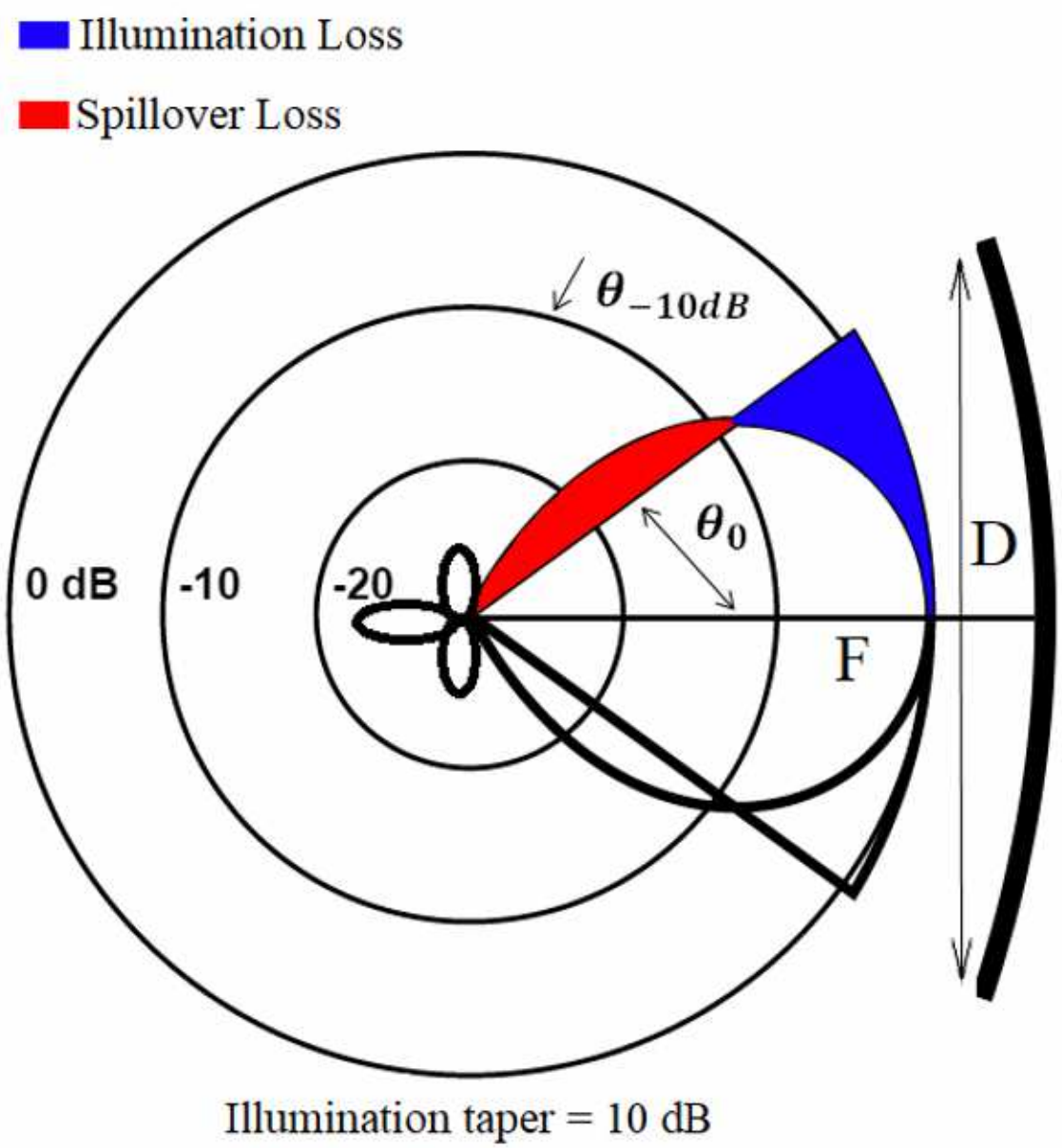

Figure 9

Spillover loss of the combined lens and horn antenna. θ0 is the opening angle of the lens, θ-10dB is the angle for -10 dB illumination taper, F is the focal length and D is the lens diameter.

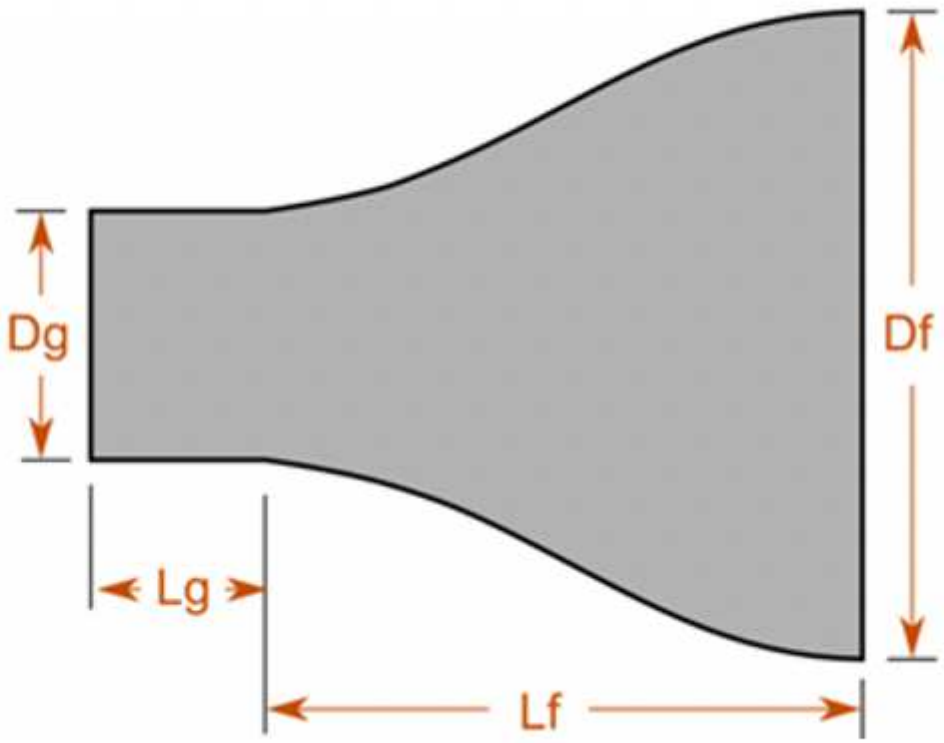

Figure 10

Schematic of the designed Gaussian profile horn with flat wall, where Dg, Lg, Df, and Lf are the waveguide diameter, waveguide length, final diameter of the Gaussian profile, and profile length, respectively.

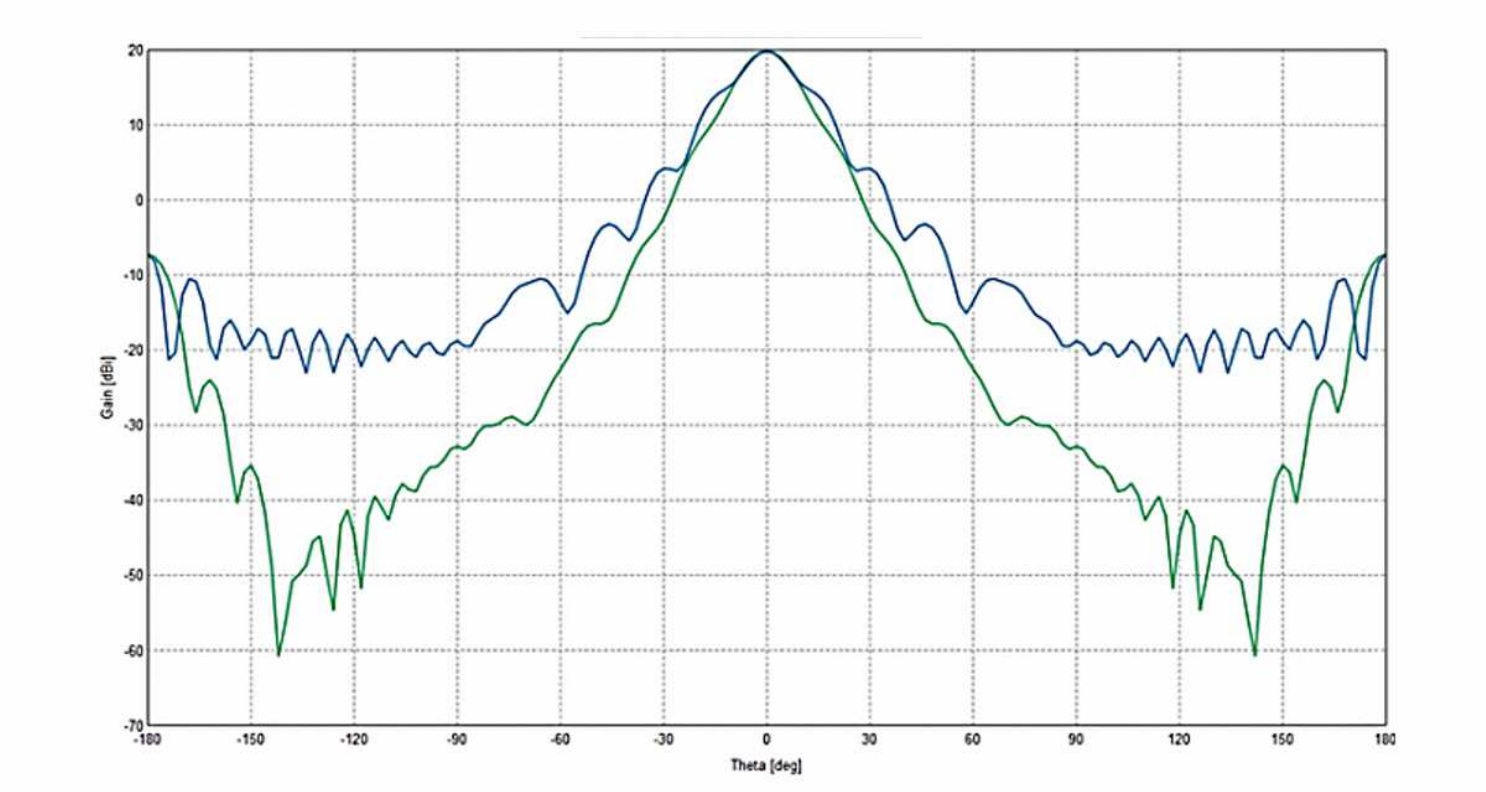

Figure 11

Radiation patterns of flat wall Gaussian profile horn at 94 GHz, in E (green line) and H (blue line) planes.

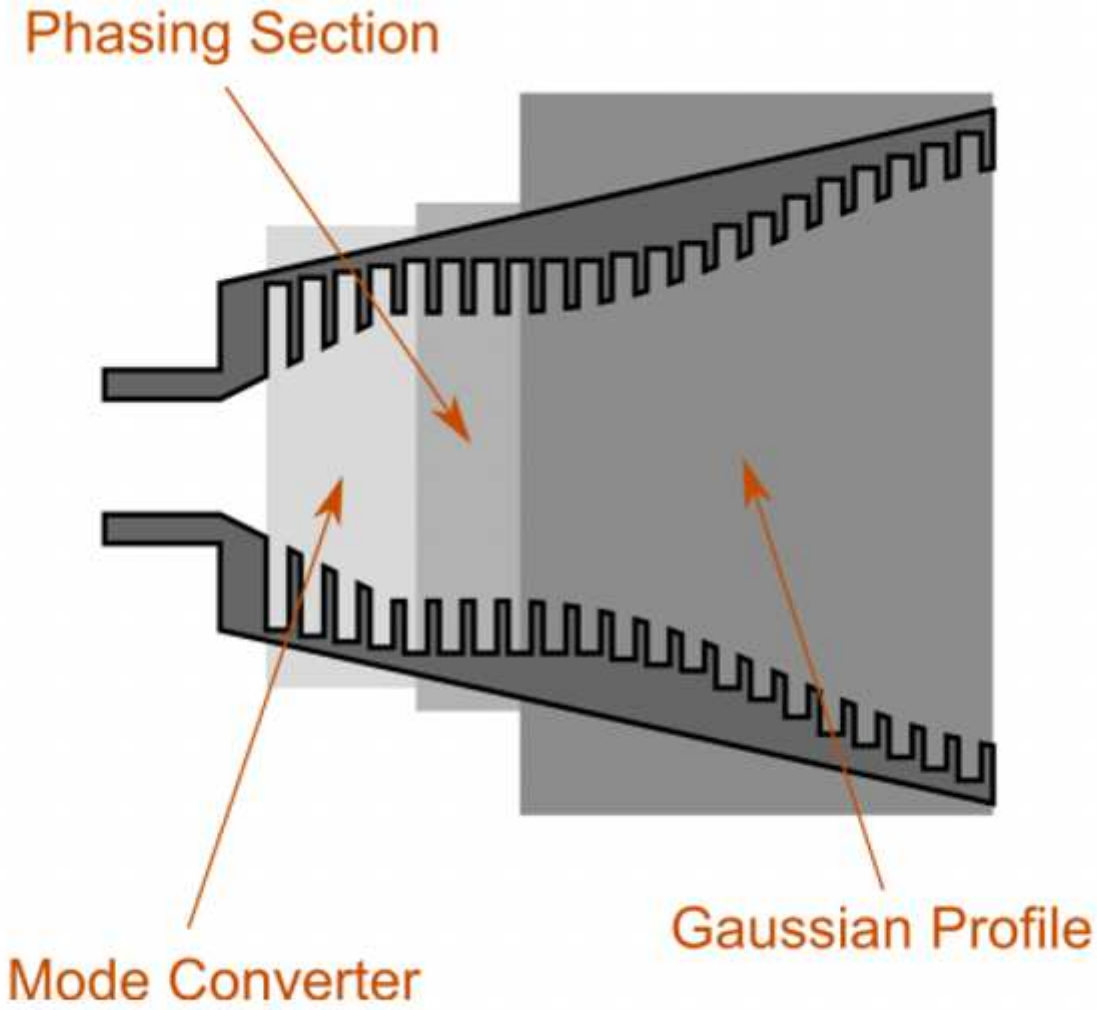

Figure 12

Schematic of the corrugated Gaussian horn.

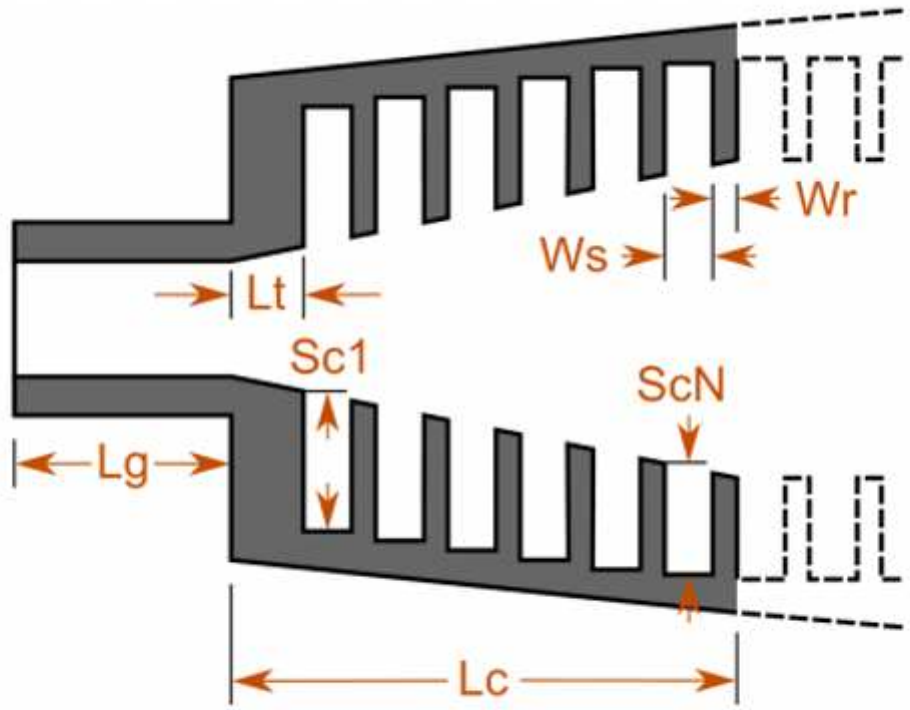

Figure 13

Mode converter with values optimized in FEKO.

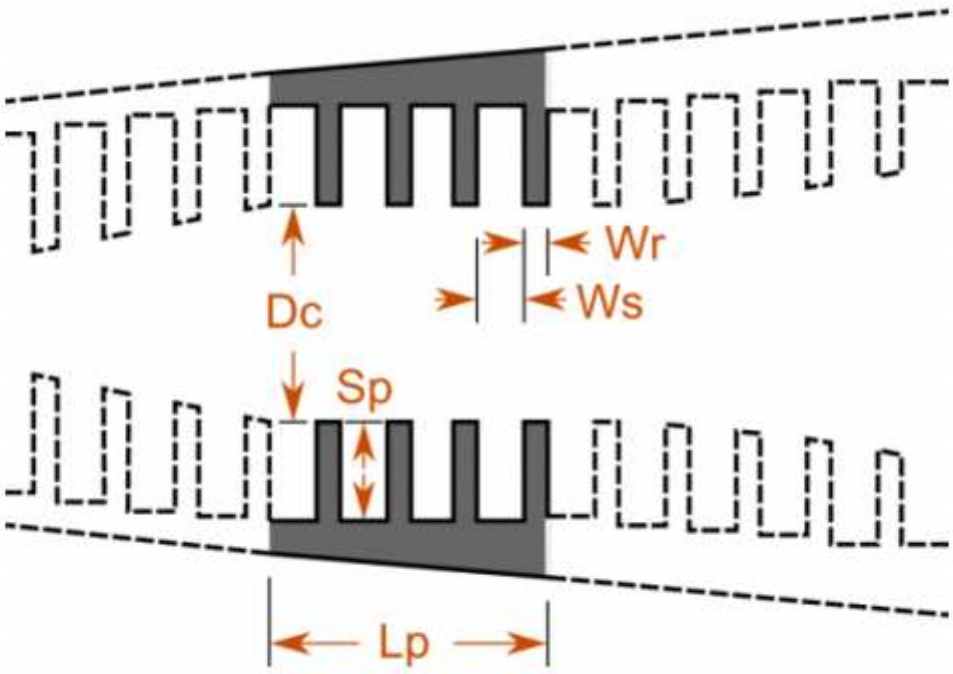

Figure 14

Phasing section in FEKO.

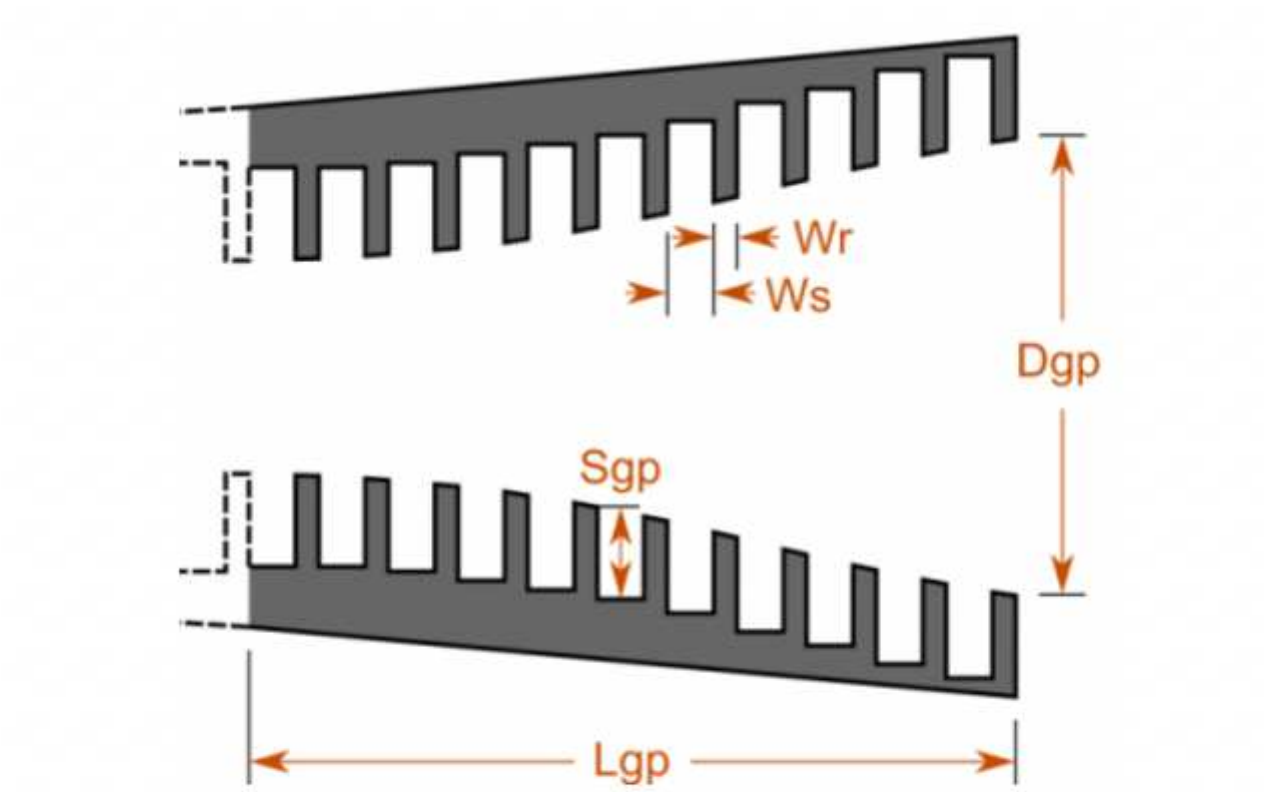

Figure 15

Corrugated Gaussian section in FEKO at 94 GHz.

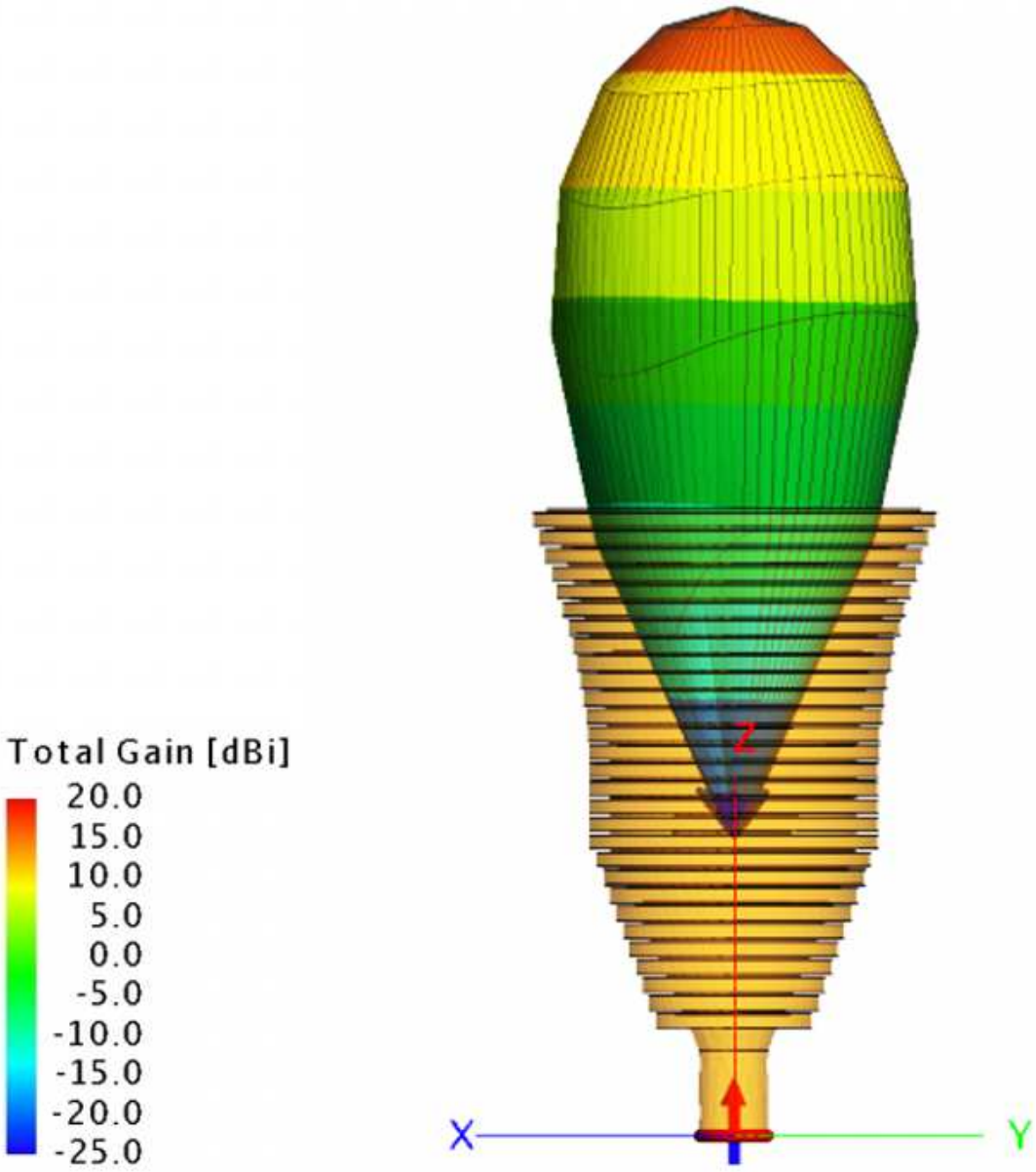

Figure 16

Radiation pattern of the designed corrugated Gaussian horn at 94 GHz.

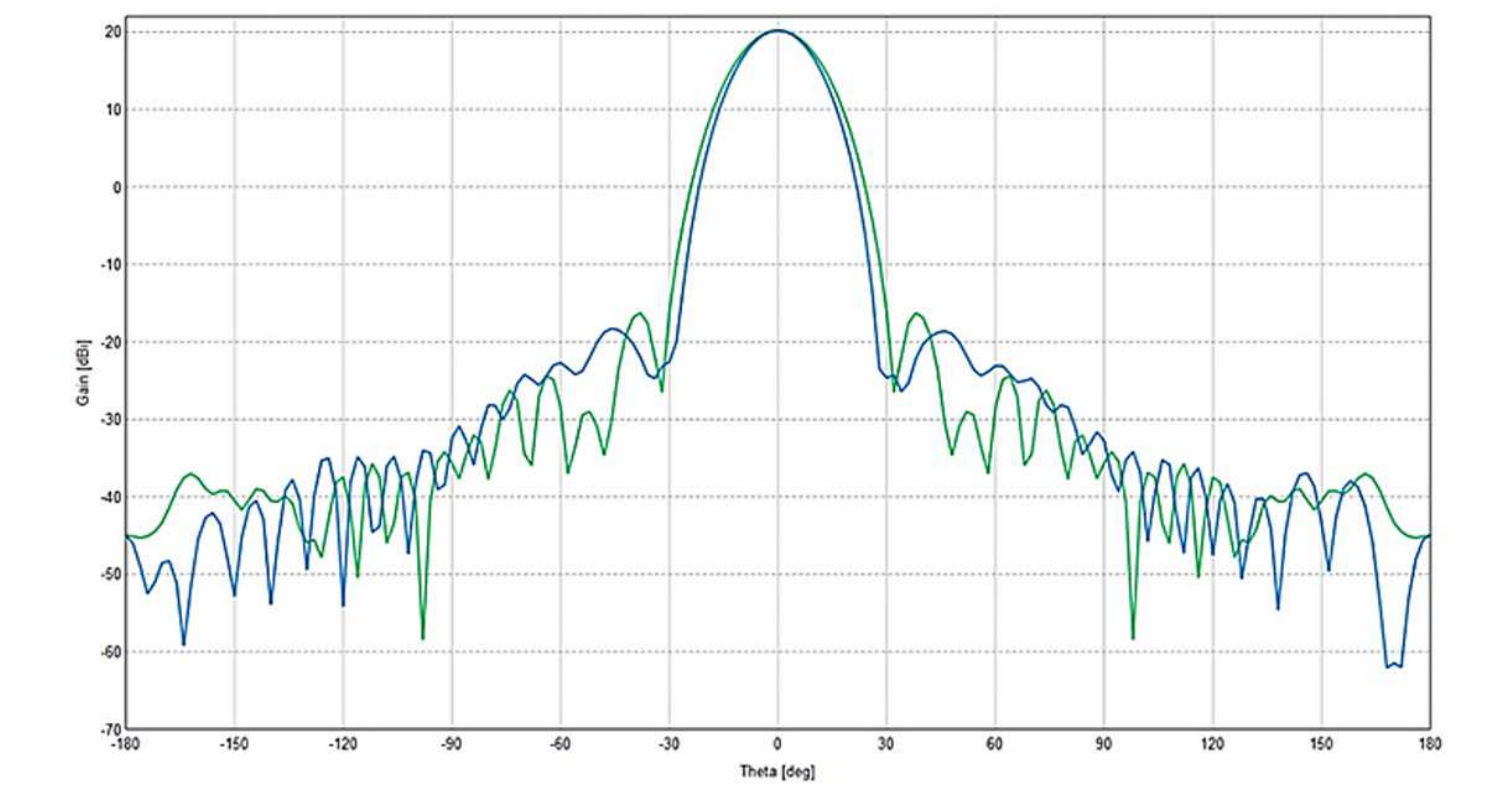

Figure 17

Far-field radiation pattern at 94 GHz in E (green line) and H (blue line) planes.